CEMENTING SLURRY SUITABLE FOR OIL AND GAS WELLBORE DRILL FOR APPLICATION IN SOUTH AFRICA

MSc RESEARCH DISSERTATION

Compiled by

Charity Dliwayo

Submitted to

School of Chemical and Metallurgical Engineering, Faculty of Engineering and the Built Environment, University of the Witwatersrand, Johannesburg, South Africa

Supervisor: Dr Diakanua Nkazi

Co-Supervisor: Dr Ralph Farai Muvhiiwa

August 2022

Declaration

I the undersigned **Charity Dliwayo (383498)** hereby declare that the work contained in this dissertation has been produced by me without collaboration with other students, staff or third parties aside from those acknowledged. I have not engaged in any acts of plagiarism and to the best of my knowledge, I have recognized all information obtained from other authors' work. This work is being submitted for the degree of Master of Science to the University of Witwatersrand, Johannesburg. It has not been submitted before for any degree or examination in any other University.

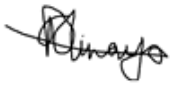

15 August 2022

SIGNATURE DATE

Abstract

South Africa's biggest local energy supply is coal, which is used primarily for generation of electricity, followed by crude oil which is imported and refined into petroleum products such as fuel for cars. In future South Africa may reduce its oil imports as there have been discoveries in oil and gas reserves in the Cape Town coastal region. Therefore, an oil rig may need to be built to extract the oil. The rig wellbore will need to be cemented using oil well cements (OWC) to seal annular space between metal casing and walls of a wellbore. OWC slurry may have reduced strength with time when subjected to environments of elevated temperatures and pressures. This study investigates behavior of two well cement slurry additives that can be used as extenders on OWC slurries. Durapozz (DZ) and Bentonite (BT) extender additives were dosed from 0-5 % by weight of cement (BWOC) at 23 and 38 degrees during compressive strength testing. The results indicated that Compressive strength at 8 h and 38 ˚C was more than twice the required value of 2.1MPa. Bentonite showed signs of losing strength over 28 days of curing at 38 degrees compared to 23 degrees, while Durapozz showed increase in compressive strength due to its good packing ability caused by the presence of a wide range of particle size distribution. However, this caused high thickening times for both additives; DZ was found to act as accelerator at low dosages and retarder at high dosages. From 0-5% Bentonite and Durapozz had approximately the same thickening times therefore BT can be substituted with DZ. The Factorial Design (FD) method was used to determine Free Fluid Content (FFC), results showed low FFC (<5.9%) as slurries are lightweight and have less than 0.44 water to cement ratio. The rheology results indicated that the Bingham plastic model best describes flow behavior of prepared slurries, and that all slurries were shear thinning with thixotropic behavior. Rheology results from drilling software indicated that flow index (n) and plastic viscosity were the same but fluid consistency index (K) and yield pressure had an acceptable error of 5-7%. Slurries prepared with BT and DZ were all lightweight slurries with densities between 1500 and 1700 kg/m3.These slurries would be applicable in low formation pressure and therefore can be cemented in conductor and surface casings less than 1800m. Significance of DZ additive density in lowering cost of slurry as well as carbon footprint was observed.

Acknowledgements

Firstly, I would like to express my gratitude to God who gave me this opportunity to conduct these investigations during challenging Covid-19 pandemic times. Glory be to him!

I want to thank my mother Jennifer and Uncle Andrew for their guidance, and moral support. Without my mother and daughter (Bathabile) support with my son's (Bukhosi) first 3 months lifetime, none of this would have been possible. A special tribute goes also to the love of my life, Andile for his support, inspiring me to never give up, always pursue excellence and their positive attitude toward my studies. To my entire family, thanks for your patience, unconditional love and support throughout this journey.

My heartfelt gratitude goes to my supervisor Dr Diakanua Nkazi without whom this research could not have been possible. Thank you for giving me the opportunity and platform to learn and explore my thoughts. To Ralph Muvhiiwa, thank you for your continued support and in-depth unique contribution throughout the duration of this research.

Special thanks go to the following companies and individuals:

Lafarge for giving me access to all the necessary resources and laboratory space to carry out my cement and additives tests; as well as provide oil well cement equivalent data from their various plants Worldwide. Particularly, I would like to thank Monwabisi Matlabyane (Laboratory Manager at PPC) for his assistance in running the tests and conducting the experiments during his time at Lafarge Cement as well as the entire Laboratory Team for providing time and space for storage of prepared samples.

Peter Wang (Global Sales Manager) from Pegasus Vertex Inc for allowing use of online 10-day Dr DE software to perform quick drilling calculations, as well as providing cementing information during their webinars; and last but not least James Z. Sun (IT Support) for dedicating his time to ensure installation of Software is done remotely via Teams Viewer.

Table of Contents

LIST OF FIGURES

LIST OF TABLES

NOMENCLATURE

Aluminum oxide	A
Calcium oxide	C
Iron (III) oxide	F
Silicon dioxide	S
Water	H
Sulfur trioxide	SO_3
Calcium Carbonate	$CaCO_3$
Magnesium Carbonate	$MgCO_3$
Calcium Silicate Hydrate	C-S-H
Tobermorite	$C_5S_6H_5$
Xonotlite	C_6S_6H
Truscottite	$C_7S_{12}H_3$
Hydrogen Sulfide	H_2S
American Petroleum Institute	API
Bentonite	BT
Durapozz	DZ
Bearden units of consistency	Bc
By weight of Cement	BWOC
Loss on Ignition	LOI
Oil well cement	OWC

Water-to-cement ratio	w/c ratio
Lime to silica ratio	C/S ratio
Compressive Strength	CS
X-ray Fluorescence	XRF

CHAPTER 1: INTRODUCTION

In these modern times, people use vehicles to be transported from one point to another. These vehicles use diesel or petrol oil to be able to move people or transport goods from one area to another. The oil is derived from crude oil, which is a mixture of hydrocarbons. The crude oil is delivered as a dark and sticky liquid, it is sent to refineries for processing by heating until it boils. As it is boiled, the liquids and gasses are separated according to boiling temperatures in a distillation column and the collected liquids from the process can be paraffin, diesel or petrol (Thetford, 2013). South Africa does not have developed oil reserves; therefore, it imports crude oil from countries such as Nigeria, Angola and Ghana who are the largest African suppliers respectively (South African Market Insights, 2020). South Africa has four refineries; Caltex refinery in Cape Town, Sapref Refinery in Durban (owned by Shell and BP), and Enref refinery in Durban owned by Engen as well as Natref refinery in Sasolburg owned by Sasol and Total (Mbedi, 2018).

The fact that oil is imported makes it expensive and the higher the price the more the country's economy struggles. In order to boost the economy of the country, one of the refinery companies, Total SA has managed to discover 3.633 km crude oil reserves in between Indian and Atlantic Ocean in Cape Town (Total News, 2019). Extraction of the oil would need an offshore oil rig to be built, which consists of a number of equipment; one of which includes drilling equipment for the wellbore.

In order for the oil drill to be successful, it is crucial to ensure that throughout the drilling process formations or rock and soil stratum does not collapse. This is done by ensuring a balance of pressures at any given time by pumping cement slurry in between the drilling casing and formations (on annulus). Cementing the annulus also protects the casings drill from corrosion and seals off water zones to avoid contamination by harmful chemicals. Therefore, it is crucial to design cement slurry that will be strong and durable. Bentonite is one of the common cement slurry additives used, this additive is expensive and its use may need to be minimized by substituting it with a cheaper additive.

1.1 Problem Statement

The compressive strength of the cement slurry is affected by type and quantity of additive as explained by Lota (1993) in his hydration of oil well cement thesis. The investigation of cement hydration was conducted at different temperatures (5 and 20 ºC) and different additive dosage; results found were that Portland cement hydrates differently from oil well cement due to its different mineralogical composition. Additives are added to Portland cement in order to slow down setting times and produce cement slurry that is comparable with oil well cements. Broni-Bediako et al (2015) did the same investigation as done by Lota (1993) comparing Ghana made cements with imported Class G cement at different temperatures for oil well cementing operations in Ghana. Their investigation highlighted that when Ghana cements were tested for fluid loss, thickening time, compressive strength, free fluid and rheology properties at 27 and 66 ºC; the tested cements were comparable with oil well cement additives and could be substituted with the imported Class G cement provided that strict quality control measures such as temperature at which specimens are stored should not change at any point during the process. Kaduku (2015) explained the use of coal fly ash from South Africa as an additive to oil well cement and he found out that slurries that contained sodium silicate synthesized from Coal fly ash had lower density, lower viscosity and high compressive strength compared to commercial sodium silicate. The setting or thickening times were unfortunately not analyzed due to a faulty instrument. This was one of the crucial elements in order to assess whether the slurry was pumpable in the annulus. The viscosity of slurry over time at different temperatures and pressure would determine the rheological characteristics of the slurry.

Due to the oil and gas reserves discovered by Total SA it is imperative to conduct more research as part of readiness if drilling plant explorations become a success. Readiness requires South Africa to be able to source most of the raw materials and equipment locally, one of which is the cementing process materials, which include the cement and additives used to make the cement slurry. Designing acceptable cement slurry that would survive the wellbore conditions requires the slurry to be able to withstand soil and rock physicochemical properties and also meet the standard API specifications. Local industries such as PPC Cement and Lafarge do produce cement that is made of clinker and gypsum only, but these are aimed for use in construction. If

these local cements are mixed with locally available additives, will the slurry survive in an oil well environment?

1.2 Research Objectives

AIM OF THE PROJECT

The aims of this project are to design and evaluate performance of clinker cement slurry that meets the API standards using durapozz, and bentonite as additives suitable for the slurry in an oil wellbore environment. The following objectives will be investigated in order to meet the aim of the project:

- Objective 1: Investigating optimum design of clinker for making class G cement using locally available raw materials and selection of design mix with minimum cost based on fuel used to burn the raw materials.
- Objective 2: To investigate optimum dosage of durapozz and bentonite additives at different temperatures and evaluating compressive strength at different curing times.
- Objective 3: To determine the movement behavior of cement slurry as it moves down the casing and up the annulus and characterize the rheological flow pattern that best fits the performance of the slurry.
- Objective 4: To compare the chemical and physical properties of a designed cement slurry using the API specification under the same environmental conditions and make a viable decision if the designed slurry would be effective in oil wellbore.

A flow diagram for the research layout is shown on Figure 1 below. To design cement with class G properties starts with the process of manufacturing the cement using specified raw materials that have designed quality parameters, one of which is high sulfate resistant cement. This cement is altered using additives in order to obtain a cement slurry that would survive wellbore conditions.

1.3 Research Work Layout

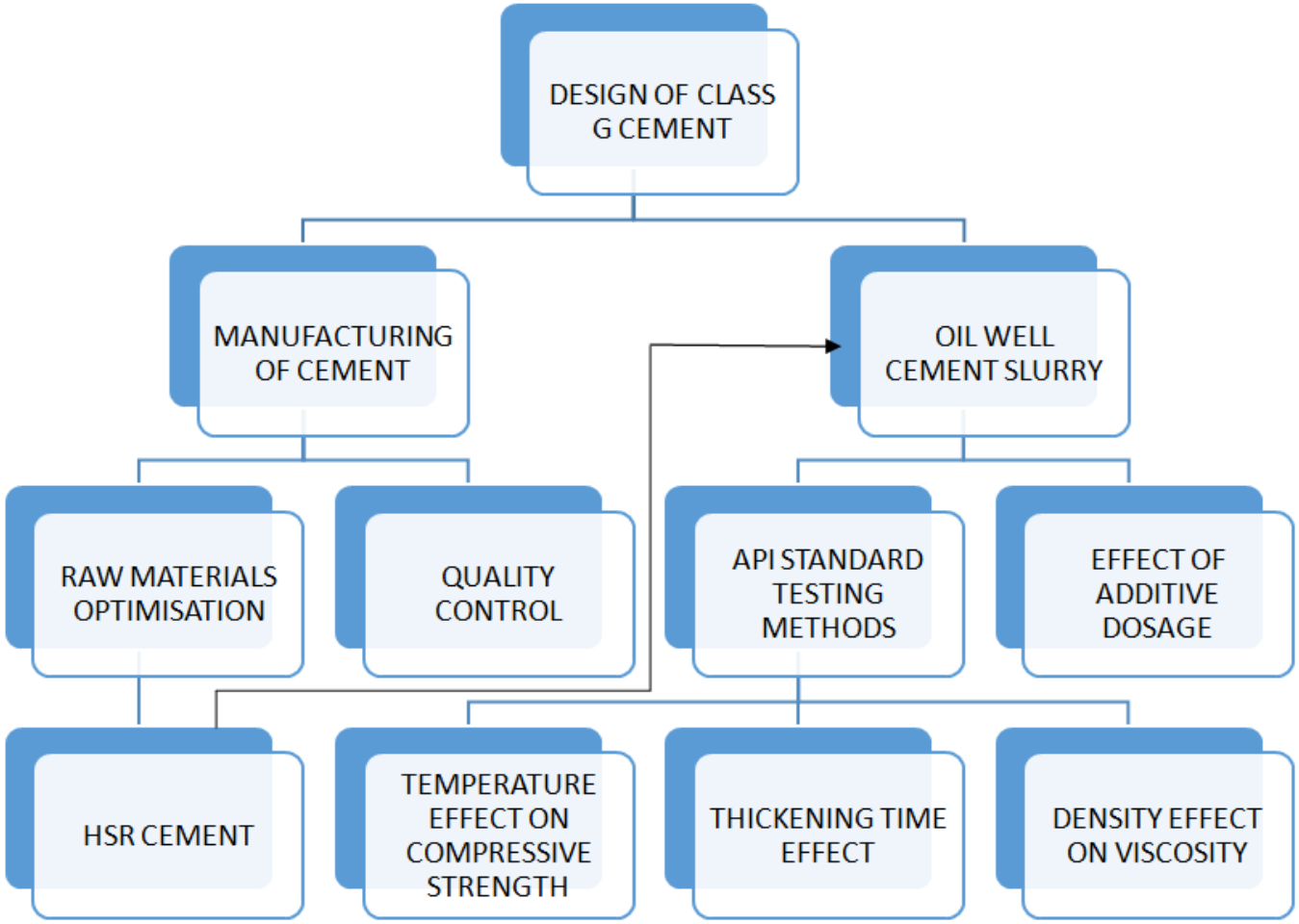

Figure 1: Research Work Layout

CHAPTER 2: LITERATURE REVIEW

2.1 Introduction

Classes of cement as recognized by the American Petroleum Institute (API), are separated by pressure, temperature and the depth of the well. The API standards are reviewed every 5 years. API standard (10 A, 24th edition) listed the six classes (i.e., Class A, B, C, D, G and H) as shown in Table 1. Class G Oil Well Cement is the most commonly used cement type in the oil and gas industry for well casing purposes due to its ability to resist sulfur attack (Guner & Ozturk, 2015).

High sulfate-resistant (HSR) and moderate sulfate-resistant (MSR) class G cements are identified by the amount of calcium aluminates. Class G cement will be the focus of this study due to its flexibility in oil well environments compared to other cement types.

Table 1.API Classification of OWCs ((Guner & Ozturk, 2015) & (Munjal, et al., 2019))

Class	Depth Range (m)	Temperature Range(˚C)	Description
A	0-1830	0-77	Used on surfaces where special properties are not important (O grade).
B	0-1830	0-77	Used on the surface when conditions require HSR or MSR.
C	0-1830	0-77	High early strength O, MSR and HSR grades suitable on this surface.
D	1830-3050	77-127	High temperature and pressure resistant MSR and HSR grades are suitable .
G	0-2440	0-93	No additives other than calcium sulfate or water, or both, shall be inter-ground or mixed with the clinker during manufacture of class G well cement available in MSR and HSR grades. Used extensively in wells of varying depths with additional additives and retarders.
H	3660-4880	0-93	Similar to class G, the difference is the surface area, Class H is coarser.

In order to design a highly performing oil well cement slurry with high durability, one needs to first understand factors that would lead to non-performing slurry during manufacturing process as well as effects to cement during transportation to drilling site. When the cement arrives at the drilling site the type of water and additive as well as its respective quantities plays an important role to the survival of slurry in downhole conditions. Therefore, the literature review will be split into following sections respectively:

1. Manufacturing of cement (How the cement is manufactured and cement quality parameters optimized for suitability in wellbore application)
2. Cement additives (Types of additives used in oil drilling and their effect on slurry properties).
3. Cementing Process (How the slurry is placed in the wellbore annulus)
4. Wellbore Conditions (How the wellbore dimensions are determined as well as calculation of estimated volume of slurry required. Detailed explanation of the wellbore environment and its effect on cement slurry).

2.2 Manufacturing of Cement

Limestone and clay materials are ground together in a raw mill to a fine powder with 12% oversize on 90 μm. The ground material is called the raw meal, this product is then stored in a homogenizing silo. From the silo, it is then carefully extracted and preheated in a series of cyclones such that 95% degree of calcination is obtained before material enters the kiln. The material is burnt at 1450 ºC inside the kiln using coal of specified quality as later shown in fuels on Figure 33. The product from kiln is called clinker. The clinker produced is further grinded with additives into a fine powder-cement also under controlled conditions. Different cements (CEM I, CEM II, CEM III, CEM IV) can be produced based on additives used to grind the cement with as well as their application. The amount of clinker used in these different cements decreases from CEM I to CEM IV, which means cement of higher quality is CEM I. In this study, focus will mainly be on CEM I, which is mainly clinker ground with approximately 3% gypsum additive (Merah & Krobba, 2017). CEM I is chosen as the main focus of study due to its highest compressive strength; other cements contain extenders such as limestone or fly ash that make cement not sulfate resistant. Figure 2 below shows a simplified flow of the process of cement manufacturing.

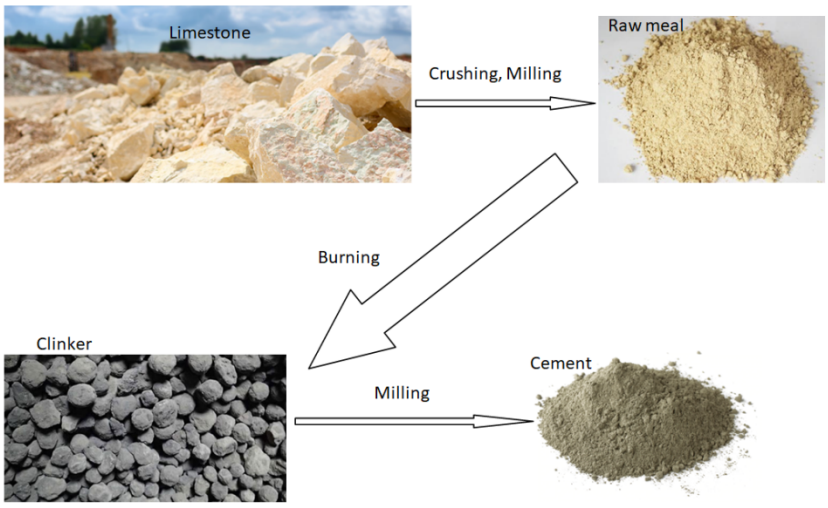

Figure 2: Typical manufacture of cement from limestone [PPC and Lafarge Plants]

The cement is then mixed with water (at a water to cement ratio of 0.44) and additives in order to make the cement slurry. The type of cement that needs to be used for oil drilling purposes needs to be medium sulfate or high sulfate resistant cement.

2.2.1 Key quality parameters for clinker

Typical lime saturation factor (LSF) range is 92-105. The higher the LSF the harder to burn the material and results in excessive free lime. LSF determined using Equation 1 below:

$$LSF = \frac{CaO}{2.8SiO_2+1.65Al_2O_3+0.35Fe_2O_3} \quad \text{.....Eq 1}$$

Typical Silica Ratio (SR) range is 1.8-2.7, Equation 2 below shows how it is calculated. The higher the SR the harder to burn the material and results in unstable coating behavior. The lower the SR the higher the liquid phase and coating becomes thicker resulting in ring formation and low 3-7 days early strength .

$$SR = \frac{SiO_2}{Al_2O_3+Fe_2O_3} \quad \text{.....Eq 2}$$

Typical Alumina Ratio (AR) range is 1-1.5, calculation is shown on Equation 3 below. High early strength in cement may be due to higher AR.

$$AR = \frac{Al_2O_3}{Fe_2O_3} \quad \text{.....Eq 3}$$

Typical Sulfur Alkali Ratio (S/A) values between 0.8 to 1.2, calculation is shown on Equation 4 below. The higher the ratio the more buildups on bottom cyclones and kiln inlet, making operation to be difficult.

$$\frac{S}{A} = \frac{\frac{SO_3}{80}}{\frac{K_2O}{94} + \frac{Na_2O}{62} - \frac{Cl}{71}} \quad \text{.....Eq 4}$$

Equation 5 or 6 is the calculation of conversion factor from when material enters the kiln to the product clinker.

$$Kiln\ feed\ to\ clinker\ factor = \frac{Kiln\ feed(kg)}{Clinker\ output(kg)} \quad \text{.....Eq 5}$$

$$Kiln\ feed\ to\ clinker\ factor = \frac{Raw\ meal\ to\ clinker\ factor\ x100}{Top\ stage\ cyclone\ efficiency} \quad \text{.....Eq 6}$$

Equation 7 is the calculation of yield value of cement from clinker.

$$clinker\ to\ cement\ factor = \frac{clinker+gypsum+flyash\ or\ slag+additive}{Clinker\ consumed(kg)} \quad \text{.....Eq 7}$$

Bogue formulas are used to calculate clinker phases (shown on Table 2) as shown on Equations 8-11:

$$C_3S = 4.071CaO - (7.602Si_2O + 6.718Al_2O_3 + 1.43Fe_2O_3 + 2.852SO_3) \quad \text{..... Eq 8}$$

$$C_2S = 2.867Si_2O - 0.7544C_3S \quad \text{..... Eq 9}$$

$$C_3A = 2.65Al_2O_3 - 1.692Fe_2O_3 \quad \text{.....Eq 10}$$

$$C_4AF = 3.043Fe_2O_3 \quad \text{.....Eq 11}$$

Loss on ignition:

$$LOI = 0.44\,CaCo_3 + 0.524MgCo_3 + \ldots + combined\,H_2O + organic\,matter \quad \text{.....Eq 12}$$

Liquid phase percentage:

$$\%\, LP = 1.13C_3A + 1.35C_4AF + MgO + Alkalies \quad \text{.....Eq 13}$$

[*Note: All formulas obtained from Cement Formulae Handbook ,published by Confederation of Indian Industry-CII - Sohrabji Godrej Green Business Center*]

Table 2: Mineralogical composition of cement clinker (Nelson, 2006)

Name	**Notation**	**Oxide composition**	**Concentration(wt%)**
Alite	C_3S	$3CaO.SiO_2$	55-65
Belite	C_2S	$2CaO.SiO_2$	15-25
Aluminate	C_3A	$3CaO.Al_2O_3$	8-14
Ferrite	C_4AF	$4CaO.Al_2O_3.Fe_2O_3$	8-12

2.2.2 Cement manufacturing optimization

Cement quality depends largely on clinker quality as well as gypsum dosage and environmental exposure._In order to obtain cement that would be used for oil well cementing, the clinker produced largely depends on raw mix optimization as well as the burning conditions in the kiln (Carruthers, 2014). Following clinker quality is aimed at:

1. Low C3A levels (<8%) for sulfate resisting properties which influence long thickening time and good pumpability and moderate to high C3S (55-65%) for quick strength development.
2. Low alkali level for long thickening time and low magnesia level to avoid strength drop and cracking.
3. Overburnt clinker with low free lime and high C_3S size to increase the thickening time (C_3S size by microscopy evaluation in the range of 50-70 µm for Class G cement). High silica sand content in raw mix and coarse kiln feed with high 90 µm residue will force the operator to overburn.

When grinding the clinker together with gypsum to make cement, following control measures need to be taken in order to produce cement suitable for oil well drilling:

1. Aim large particle size distribution (25 mm) and low to moderate fineness (400-420 m^2/kg Blaine surface area) to increase thickening time and reduce viscosity
2. Aim SO_3 content below 3% in order to avoid over sulfating, which leads to longer thickening time. Under sulfating will cause short thickening time and poor workability. Use of natural gypsum is advised as opposed to artificial gypsum, which may tend to have chemicals that interact with additives.
3. Control of gypsum dehydration is important for product performance. There must be a balance between the soluble sulfates in controlling hydration to avoid high amounts of hemihydrates, which can cause short thickening times. Cement mill outlet temperature is normally maintained below 115 ˚C to avoid gypsum dehydration, which occurs above 130 ˚C (Tang, et al., 2019).
4. Cement is stored in silos with temperatures of 60 to 80 ˚C to avoid lump formation, strength drop as well as poor compatibility with additives (Carruthers, 2014).

The cement slurry to be used for oil drilling needs to meet the American Petroleum Standards, as specified on Table 3 :

Table 3. API Standard -Properties of class G cement (Nehdi, 2012; Nelson, 2006 & Rzepka, et al., 2016))

Chemical Component	**%**	**Physical Properties**	
SIO2	21.6	Fineness 45 μm sieve	92.4% passing
Al2O3	3.3	Blaine	385 m^2/kg
Fe2O3	4.9	Thickening time at 52 ºC and 36.5 MPa	90-120 min at 100 Bc 15-30 min at 30 Bc
Total CaO	64.2	Compressive strength at 8h at 38 °C	2.1 MPa
MgO	1.1-6	Compressive strength at 8 h at 60 °C	10.3 MPa
SO_3	2.2-3	Maximum free water content	3.5 mL or (5.9% after 2 h)
Loss on ignition	0.6	Density	1900 kg/m3(1400-2300 kg/m3 accepted)
Insoluble residues	0.3-0.75		
Equivalent Alkali (Na_2O)	0.41-0.75		
C_3A	1-5		
C_3S	50-65		
C_2S	15-30		
C_4AF	12-15		

2.3 Cement Additives

Cement properties are adjusted using additives in order to get the quality of slurry suitable for an oil well drill. The additives increase or decrease the density of the cement. The need for density decrease is accompanied by easy pumpability of the cement.

Apart from the common mentioned additives (Table 4), there are also additives used in the removal of leakage of drilling mud or cement slurry as well as additives used for anti-pollution. It is also important to note that the additives do not remain as one type, and type depends on dosage and also some can fall on different types at the same time. For example, little salt will accelerate but more salt will retard the cement (Nelson, 2006).

Table 4. Additives used for oil well cement slurry (Bennett, 2016 & Bett ,2010)

Type	Purpose	Examples
Accelerators	Speed up hydration and reduce thickening times	Calcium chloride (1-3%), Gypsum, Sodium chloride (2-2.5%)
Retarders	Slow down thickening time	Sugar, sodium chloride, lignosulfonate (0.1-5%).
Extenders	Decrease density	Bentonite (2-16%), gilsonite, kolite, foamed cements
Weighting Agents	Increase density	Hematite, sand, salt
Dispersants	Reduce viscosity	Friction reducers

2.4 Well Condition

There are generally two major decisive factors for the design of cement slurry:

1. Depth and dimensions of the well
2. Environmental conditions of the wellbore which include formation type, salts presence, drilling fluid, as well as temperature and pressure gradients (Carruthers, 2014).

Well depth and dimensions

The design of a well begins when the production zone has been located, which in turn gives the overall depth of the well. The rate at which the oil or gas will be extracted determines the diameter at the bottom of the hole and the successive casings above the production zone depend on drilling requirements or geological considerations (Finger, 2010). Multifinger caliper logs are used to simultaneously measure the diameter of the wellbore along its depth at different points so as to take into account any irregularities in the wellbore diameter (Crook, 2006). The amount of slurry to be injected per casing can now be determined by subtracting whole volume from casing outer volume as shown below:

For conductor casing, slurry volume, is calculated as follows:

$$V1 = 15\ x\ \frac{\pi}{4}(1.02^2 - 0.914^2) \quad \text{..... Eq 14}$$

$=2{,}415\text{m}^3$

Geothermal wells are cemented from bottom to surface while most oil and gas wells cementing only takes place at the bottom with finishing fluid between the rest of the casing and wellbore wall. The placement of cement between the casing and the formation (annulus of the wellbore) is important to provide mechanical support to the casing especially under different temperature changes and also to protect the outside casing from formations and its corrosive fluids (Finger, 2010).

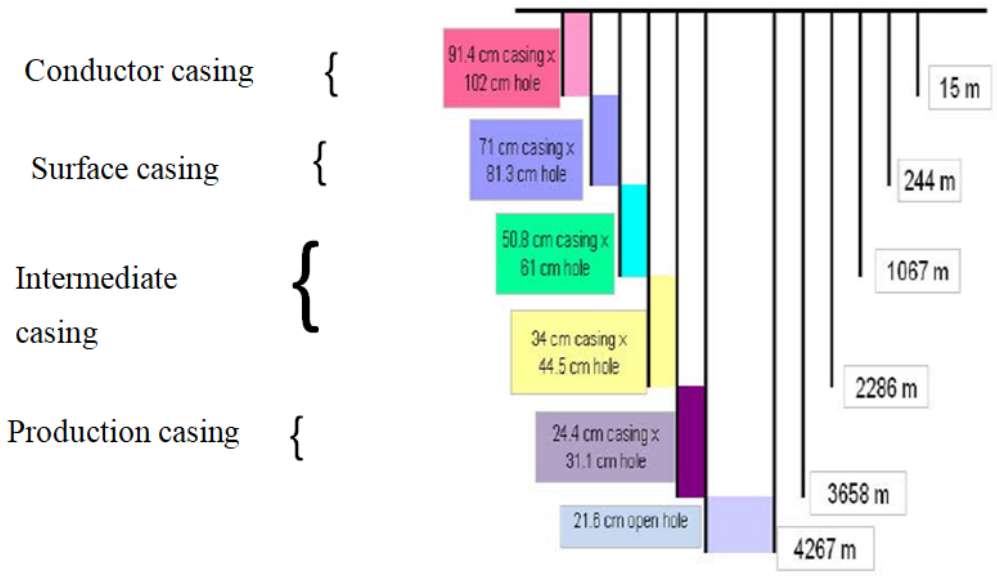

Figure 3. Geothermal well (Finger, 2010)

Figure 3 above shows a geothermal well with different size casings as well as depth of the wellbore, each casing reason for cementing is described as follows:

1. *Conductor casing* is cemented to keep away the exterior steel from wearing away caused by drilling fluids flowing outside the casing up the annulus.
2. *Surface casing* is cemented to keep away organic compounds from moving into ecological zones where salt concentration is low.

3. *Intermediate casing* is cemented to separate formation which may fracture and cause fluids to leak into the well. In most cases this casing is usually the longer casing or can be short but doubled.
4. *Production casing* is cemented to stop hydrocarbons moving to their zones and to avoid the fall down of formations causing a drop in output (Crook, 2006).

2.5 Wellbore Environment

Cement slurry's critical role is to isolate the rock formations from the well bore by acting as a seal that would stabilize both the rock formations and the casing drill in a wellbore (Pikłowska, 2017). Criteria used to choose the cement slurry that would be used in a wellbore depends on the physical and chemical compatibility of the slurry with the environment; and how tight the cement slurry is to avoid air or liquid leakages. In addition, the strength and durability of the cement slurry as well as how harmful the slurry is to the ecosystem, and also the amount of money spent when using this slurry are decisive factors.

Below are the environmental conditions in which the cement slurry will be exposed to and the slurry property required in order for the slurry to fit the conditions of the wellbore:

2.5.1 Variable temperature increases

Temperatures in the wellbore can rise to as high as 380 °C. It is important to make sure that the quantity of heat given off during the cement slurry bonding reaction should be kept at a narrow range due to the different expansion of steel and hardened cement, failure to control this would result in a leakage (Pikłowska, 2017).

2.5.2 Wellbore and pumping pressure

The pressures can rise to about 200 MPa. The density of the cement slurry should rely on the geological environment that exists. When the cement slurry is applied, it is important to make sure that it exerts the pressure that would stabilize the rock formations as well as casing drill (Pikłowska, 2017). The nature of resulting hardened cement is identified by appropriate strength parameters, corrosion resistance and stability with rock formations and casing columns. The minimum tensile strength required to maintain the suspension of the casing tube is 560 kPa,

which corresponds to a crushing strength of 700 kPa (Pikłowska,2017). Consistency and pumping time of the slurry will guarantee survival of the slurry under the existing environment in wellbore. The slurry should quickly bind after pumping (Pikłowska, 2017).

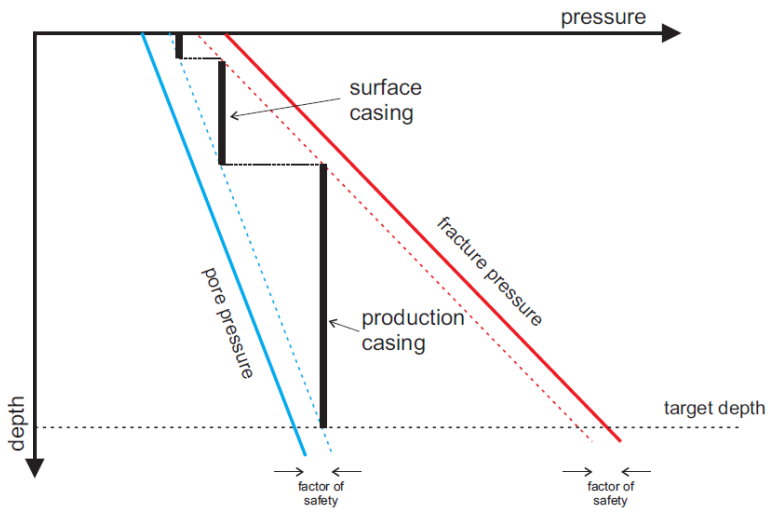

Figure 4. Well design balance of pressures (Benett, 2016)

Figure 4 above shows how the formation pressure window between pore and fracture pressures greatly influences necessary mechanical design of the well. If well pressure becomes lower than pore pressure there is risk of kicks or blow outs. If well pressure becomes higher than fracture pressure there will be loss of circulation (Pinka & Kucirkova, 2015). A safety factor is therefore, implemented to avoid such disastrous incidents. A well cement location simulator is used to additionally check pore and fracture pressures of the formation to guarantee that no challenges will be encountered in dynamic pressure throughout pumping of cement (Bennett, 2016).

2.5.3 Effect of salt water on slurry

Water produced from the oil extraction process comprises formation water, mixture of injected water, hydrocarbons as well as hydraulic fracturing chemicals. This water may have composition as in Table 5 below (Pichtel, 2016). Additives as shown in Table 4 can be used to account for the reactivity of some of the chemicals found in water that can affect the effectiveness of the cement slurry.

Table 5. Composition of water produced from an oilfield (Pichtel, 2016)

Parameter	Range	Metal	Range(mg/L)
Density(kg/m^3)	1014-1140	Ca	13-29.222
Conductivity(µS/cm)	4200-58600	Na	132-97 000
Surface Tension(dyn/cm)	43-78	K	24-4 300
Turbidity(NTU)	182	Mg	8-6 000
pH	4.3-10	Fe	<0.1-100
TOC(mg/L)	0-1500	Al	310-410
TDS	267 588	B	5-95
TSS(mg/L)	1.2-10 623	Ba	1.3-650
Dissolved oxygen(mg/L)	8.2	Cd	<0.005
Total Oil(mg/L)	2-565	Cu	<0.02-1.5
Volatiles(mg/L)	0.39-35	Cr	0.02-1.1
TPH(mg/L)	>20	Li	3-50
Chloride(mg/L)	80-200 000	Mn	<0.004-175
Bicarbonate (mg/L)	77-3990	Pb	0.002-8.8
Sulfate(mg/L)	<2-1650	Sr	0.02-2.204
Sulfite(mg/L)	10	Ti	<0.01-0.7
NH_3-N(mg/L)	10-300	Zn	0.01-35
Phenol(mg/L)	0.009-23	As	<0.005-0.3
Volatile fatty acids(mg/L)	2-4900	Hg	<0.005-0.3
		Ag	<0.001-0.15
		Be	<0.001-0.004
		Ni	<0.001-1.7

Sodium chloride (Salty water) is the main constituent of the water produced from the oilfield. Lower salt concentrations accelerate the hydration process of the cement slurry, and higher salt

content retards the hydration process. The selected slurry needs to be resistant to erosive / or aggressive action of reservoir waters (Pikłowska, 2017).

Effect of methane and hydrogen sulfide gasses

Hydrogen sulfide gas has an effect of increasing permeability of the cement slurry since they are corrosive and destroy the entire structure of the cement slurry. Gasses can migrate along the annulus, between cement and casing or formation; also, it can attack the liquid slurry due to less hydrostatic pressure or during cement hydration. Therefore,there is a need to ensure proper removal of mud, prevent or counteract mechanical stresses and also design gas tight slurry with no free water content (Pikłowska, 2017). Therefore, the cement slurry chosen needs to be sulfate resistant

2.5.4 Effect of wellbore soil and rock profiles

The designed cement slurry needs to be harmless to the rock and soil profile environment and vice versa. As the cement slurry interacts with the rock and soil profile, fluid may migrate to the formations causing damage to formations (Nelson, 2006). Higher cement slurry pressure in the annulus may fracture the formations as well as low hydrostatic pressure, a balance in pressures need to be maintained in order to avoid loss circulation. Cellophane flakes and fibers made from glass can be used to prevent loss circulation by adding them in cement slurries.

Table 6. Different Rock profiles(Mayne, 2018)

Sedimentary			**Metamorphic**		**Igneous**	
Grain Aspects	**Clastic**	**Carbonate**	**Foliated**	**Massive**	**Intrusive**	**Extrusive**
Coarse	Conglomerate	Limestone	Gneiss	Marble	Pegmatite	Volcanic
	Breccia	Conglomerate			Granite	Breccia
Medium	Sandstone	Limestone	Schist	Quartzite	Diorite	Tuff
	Siltstone	Chalk	Phyllite		Diabase	
Fine	Shale	Calcareous	Slate	Amphibolite	Rhyolite	Basalt
	Mudstone	Mudstone				Obsidian

Table 6 above shows different rock profiles that can be encountered when drilling a wellbore, these can be cut by different drills as igneous is harder than sedimentary and found in deeper wells (Mayne, 2018). Sedimentary rocks have softer material that has moisture and can react with cement slurry, this is accounted for by choosing drilling fluid, spacer, and cement slurry that is compatible with the clay minerals from the formations, this provides stability to the wellbore (Nelson, 2006). Formations may also have ice water solids and carbonic gas hydrates, which are steady only in environments of high pressure and low temperature; these tend to melt and interact with the cement slurry, an example of this is H_2S gas as explained above.

2.5.5 Effect of drilling mud and its chemical impact

Contamination of some drilling mud additives may absorb cement particles and agglomerate causing the slurry to be less pumpable. In order for the cement slurry to be stable it needs to be homogenous all the time, such that low fluid loss, porosity and viscosity is monitored which in turn provides effective displacement of mud from the well (Pikłowska, 2017).

2.6 Process of Cementing

Once the required additive is selected, it is then used to alter the slurry characteristics by mixing it with cement and water. Blending and mixing is much easier if bulk handling is practiced. Ensuring there is enough water for mixing the slurry as well as ensuring the water does not have any contaminants is a priority (Bett, 2010).

The casings and its centralizers as well as float collar, guide or float shoe is placed in the hole until the shoe is about 500 to 700 m away from the well base (Figure 5). Top of the casing string is then joined with the cementing head. Cementing head consists of wiper plugs and inlets for feeding of cement slurry, spacer fluid and drilling mud.

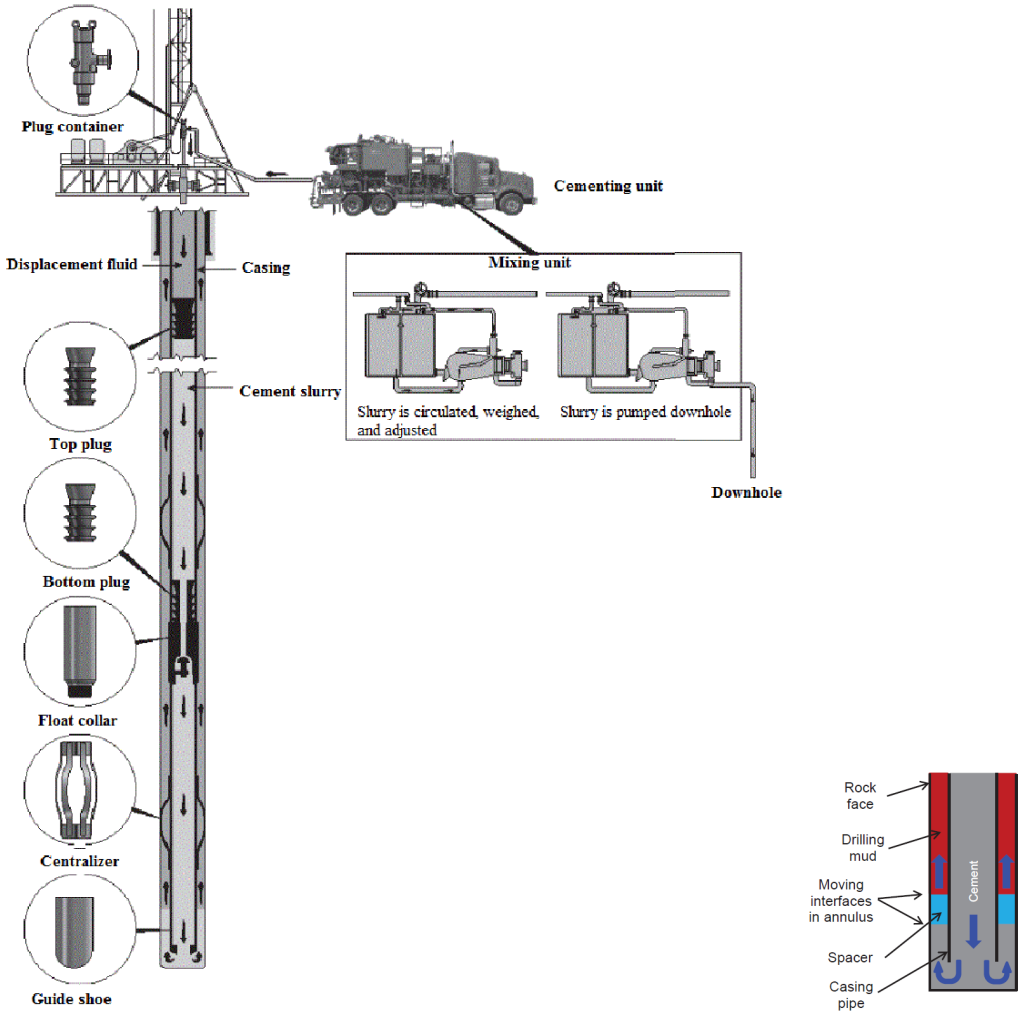

Figure 5. Procedure for cementing (Bett, 2010) and fluid movement during cementing (Lavrov, 2016)

Pressure test of all high-pressure lines with water before pumping any fluid into the casing is necessary in order to verify maximum acceptable pressures, which should be a minimum of 69bar below test pressure. The casing is then rotated clean with drilling mud prior to commencement of the cement operation (Bett, 2010). The bottom (wiper) plug is released down the casing and forced down to clean the inside of the casing. The Spacer fluid is then injected before the cement slurry so as to avoid the drilling mud from mixing with the cement slurry. By the time the bottom plug touches the float collar, its latex diaphragm ruptures. This permits the spacer fluid and cement slurry to move through the plug, around the shoe and up the annulus. The upper wiper plug is then freed, subsequently displacing fluid is pumped (Bett, 2010). When

the upper plug reaches the float collar, it sits on the bottom plug and this ceases the displacement process. As the top plug nears the float collar pumping rate should be decreased. As the cementing process progresses; it is important to make sure that the formation has not collapsed, this is done by analysis of mud returns from the annulus. If there is breakdown of formations the rate of mud extraction will be low or ceases. The cement is kept intact by the positive seal in the float collar and shoe and thus will not return back up. Valves at the casing head must not be shut off when one waits for cement to set, this is done so as to release the pressure increase caused by increase of fluid temperature which expands the casing (Bett, 2010).

For the cement to be covered all around the casing it is important that the casing pipe is centralized. This is usually done by installation of centralizers per section pipe length. Casing eccentricity is essential to avoid cement channeling through the mud (Bennett, 2016).

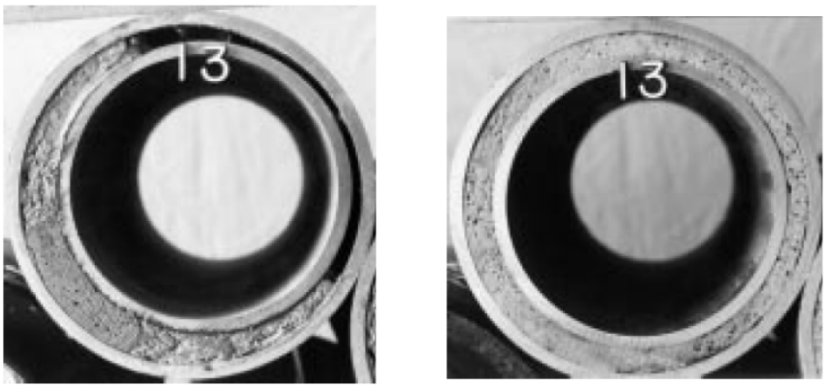

Figure 6. Mud channeling during cement placement, a) low stand-off, b) good placement (Bennett, 2016)

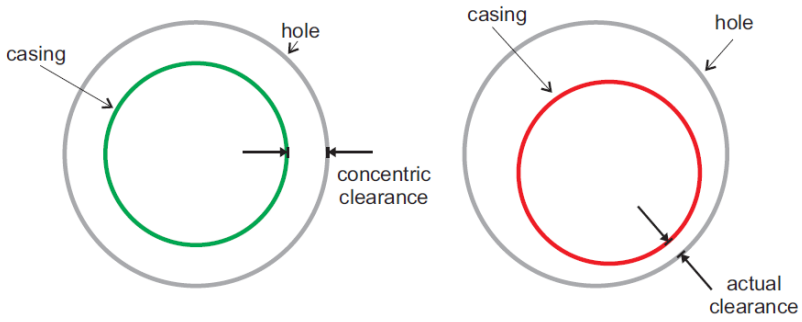

Figure 7. Schematic of STO (Bennett, 2016)

The casing eccentricity is denoted by the casing stand-off (STO) as displayed on Figure 6 and 7 above. A 100% STO implies that the casing is perfectly centralized in the open hole (OH) and 0% implies that the casing is touching one side of the formation. The lesser the STO, the more challenging it is to take out the mud on the thinner side of the wellbore annulus and the higher the threat of cement channeling through the mud on the wider side of the annulus as shown in figure above. Minimum accepted STO is 70-75%, calculation of STO is shown on Equation 15 below (Bennett, 2016).

$$STO = \frac{Actual\ clearance}{Concentric\ clearance} x100 \quad \text{.....Eq 15}$$

In order to support the wellbore formation pressures, mud and cement slurry provide the hydrostatic pressure along the depth of the well. If the mud weight is too low compared to the stress that the wall of the wellbore is exerting, the borehole will collapse. Mud weight plays an important role in ensuring that no loss in circulation or wellbore instability occurs during cementing operation and drilling activities (Aird, 2019). Density of cement slurry needs to be greater than density of spacer fluid, and density of space fluid needs to be greater than density of mud (Bennett, 2016). This ensures stability on both formations and cementing operations. The spacer fluid is there to avoid contamination between mud and cement slurry.

While the cement is being pumped in the wellbore annulus, it can exhibit different flow patterns that are based on physical properties of the slurry, its velocity as well as channeling geometry. These flow patterns are illustrated in Figure 8 below. Turbulent flow is mostly preferred but difficult to attain due to limitations caused by irregular wellbores as well as non-eccentric annuli, in such cases friction reducers are added to get a more turbulent flow. (Bett, 2010).

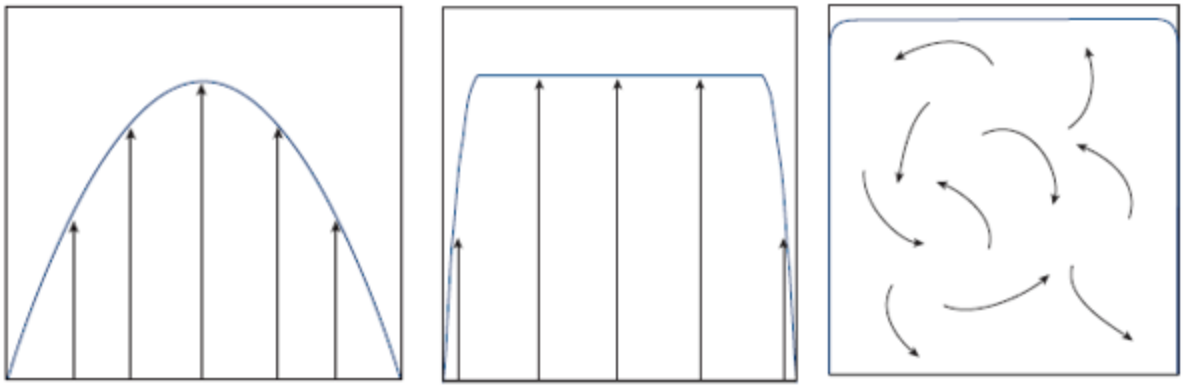

Figure 8. Lamina, plug and turbulent flow (left to right) (Nelson & Dominique, 2006)

The annular displacement rate is usually between 1.2 -1.8 m/s in order to obtain higher displacement efficiency. If a challenge is encountered plug flow is conducted in wellbore annulus at low velocities of 0.15-0.45m/s (Bett, 2010). Laminar flow is not ideal for cement slurries due to the fact that some slurry particles will adhere on the walls of piping and not move, this will create risk of blockages or cement not being pumpable up to the surface (Nelson & Dominique, 2006).

CHAPTER 3: EXPERIMENTAL METHODS AND TECHNIQUES

3.1 Introduction

The research project will be done by laboratory testing of properties of the developed cement using standard procedures from American Petroleum Institute Recommended Practices (API RP 10B) which is equivalent to ISO 10426-2. Cement slurry preparation compressive strength and thickening time testing procedures were obtained from British Standards (BS EN 196-1 and 196-3 :2005 respectively). For experiments that could not be completed due to Covid-19 restrictions, a factorial design method was used.

3.2 Laboratory Testing

As mentioned, the project can be a success by either using the laboratory facilities to test for slurry properties or using a model to access wellbore conditions suitable for the cement slurry. Materials used and their suppliers are shown on Table 7 below. The challenge with basing the research on laboratory work only was the availability of all the equipment required to conduct the tests as well as the national restrictions on Covid 19 pandemic.

Table 7. Materials Required

Slurry property	Material/Equipment required	Supplier
All	Portland Cement	Lafarge Lichtenburg Cement
Effect of additive dosage	25kg Bentonite	G&W Base and Industrial Minerals
Effect of additive dosage	Durapozz	Lafarge Lichtenburg cement
Slurry mixing	Blender/mixer	Lafarge Lichtenburg Cement
Slurry density	Mud balance or Scale weighing	Lafarge South Africa
Thickening time	ToniSet	Lafarge Lichtenburg Cement
Compressive strength	Compression Tester	Lafarge Lichtenburg Cement
Rheology	Viscometer	Lafarge Lichtenburg Cement

Bentonite was bought for R125/25kg -All other materials supplied free by Lafarge

3.3 Cement Slurry Preparation

Previous studies have shown that cements with higher water content lose strength easily and become less durable because of the decrease in volume fraction of solids. Therefore, it is recommended to use water to cement ratios between 0.3 and 0.5 (Nehdi, 2012). Water to cement ratio of 0.44 is recommended for class G oil well cement. Because of moisture in additive materials, the water to cement ratio used for experiments was less than 0.44. The w/c ratio required also depends on the fineness of material. It is important to blend all solid mixtures before adding the liquid so that the material becomes homogenized and uniform. The Durapozz sand and Bentonite additives will be mixed independently with cement prior to water addition. Bentonite addition ranges from 2 to 16% by weight of cement (Bett, 2010). In this study

Bentonite will be substituted in cement from 0 to 5% respectively. Durapozz is a silica containing material and will be substituted at 0 to 5% BWOC (Broni-Bediako, et al., 2016). The chemical composition of materials (shown on Table 8 and Figure 9) was analyzed using the XRF instrument .

Table 8. Chemical Composition, Source and Size of Bentonite, Durapozz and Cement

Chemical	Durapozz	Bentonite	Cement
SiO2	50.6	55.69	20.88
Al2O3	30.6	18.41	4.93
Fe2O3	4.63	6.35	3.3
CaO	4.65	2.87	65.24
MgO	1.06	3.54	2.29
K2O	0.6	0.58	0.15
Na2O	0.12	3.24	0.24
LOI	0.42	8.49	0.1
Moisture	11.3%	8-15%	<0.5%
Density	1100 kg/m^3	1000 kg/m^3	2800 kg/m^3
Particle Size	6-12% oversize on 45 µm	<5% oversize on 150 µm	0.4% oversize on 45µm
Supplier	Ash Resources Pty Ltd	G & W Mineral Resources	Lafarge Cement 52.5 N

Figure 9. Extenders i.) Bentonite powder(left) & ii.) Durapozz (right) Additives [Lafarge Cement Plant]

3.4 Slurry Density

The procedure uses a pressurized fluid density balance. Slurry is transferred into the cup and a pressure cap is attached. A pressurizing plunger packed with slurry (comparable in procedure to a syringe) is attached to the cap, and pressure is exerted to break down air bubbles incorporated in the slurry. Then the device is positioned on a pivot, and a downhill load is modified until both sides are balanced (Nelson, 2006). In case, if the mud balance is unavailable, a traditional method is used. This is done by measuring the mass of slurry in a known volume of container, alternatively density of slurry can be calculated if density of individual solids is known as well as concentration of solids in slurry is known.

3.5 Fluid Loss Control

After conditioning in an atmospheric consistometer the slurry is then poured in a static heated cell (shown on Figure10) of 6.9 MPa differential pressures (Hossain & Al-Majed, 2015). Filtration is achieved by collecting the filtrate after 30 min from a cylinder and using 44 μm sieve jagged on 250 μm such that residual collected covers 22.6 cm^2. The volume of liquid filtrate collected is recorded and then multiplied by two for reporting purposes (Nelson & Dominique, 2006).

Figure 10. Static pressurized heated cell (DeBruijn & Whitton, 2021)

In some instances, filtrate is collected within 30 min. This case requires loss of fluid to be determined as follows using Equation 16 (Nelson & Dominique, 2006).

$$Q_{30} = Q_t \frac{5.477}{\sqrt{t}} \quad \text{..... Eq 16}$$

Where,

Q_{30} = volume of filtrate (mL) obtained within 30 min

Q_t = volume of filtrate (mL) obtained at time *t* (min).

t = time measured in minutes

This experiment was not conducted due to unavailability of equipment and as well as strict Covid-19 regulations.

3.6 Free Water Content

Water may separate from the slurry if it is permitted to stand for prolonged time prior to setting as shown on Figure 11. The free-fluid 2 h test measures the tendency of water separating using a graduated cylinder. The procedure allows slurry conditioning at higher temperatures and pressures. For temperatures less than 80 °C, the graduated tube is placed in a preheated or precooled test chamber (Nelson & Dominique, 2006).

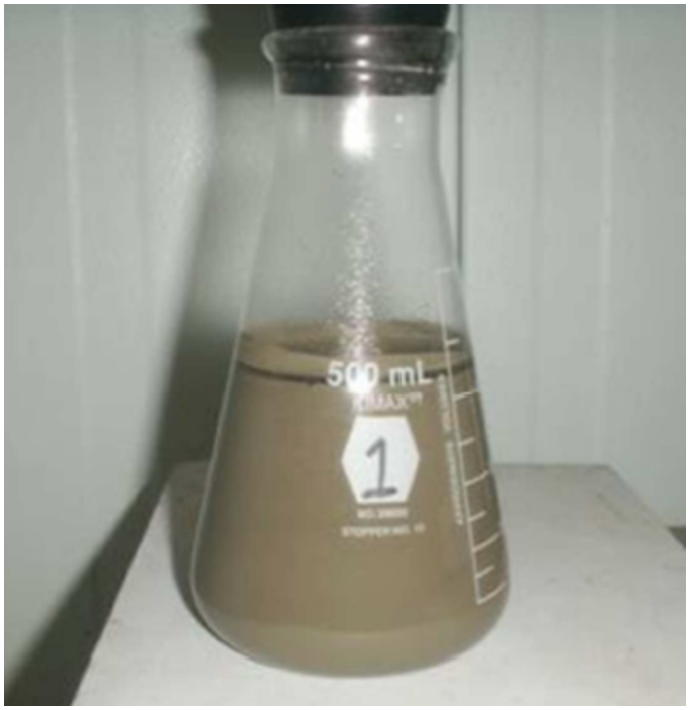

Figure 11. Free water determination

After a suitable conditioning period, the slurry is transferred into a sedimentation tube shown on Figure 12. The full tube of slurry is put in a water bath that is heated to 90 degrees. The slurry temperature is then altered to duplicate temperature variations in the wellbore. After a suitable curing time of 24 h, the set cement is divided into numerous parts (Nelson & Dominique, 2006)

Figure 12. Segmented test tubes

The density of each section is measured, and the difference in percent density of liquid and set samples is calculated using the following equation 17:

$$\Delta\rho = \frac{\rho_{cem} - \rho_{slurry}}{\rho_{slurry}} x100 \quad \text{Eq 17}$$

Where;

ρ_{cem} cement segment is density

ρ_{slurry} cement slurry density

For this study, a factorial design (FD) method was used to get the free fluid content (FFC).

3.7 Compressive Strength

450 g of cement was weighed and added in a 5 L mixing bowl, then 250 mL of water was added. Mixing bowl with the contents was then placed in the mixer machine, which was started at a low speed of 140 rpm as shown on Figure 13. Mixer then switches to high speed (285 rpm) and continues mixing for 60 s. All mixing was conducted at a room temperature of 23 °C (Nehdi, 2012).

Figure 13. mixing bowl in action(left) and mold filled with paste (right)

Mold the specimens immediately after preparation of mortar into 40 X 40 X 160 mm prisms as shown on Figure 13. Cover mold with a glass plate and seal rubber around edges of mold, and then place in the cabinet for 24 h as illustrated on Figure 14.

Figure 14. mold covered and labeled(left), controlled cabinet (right)

Plastic hammer is used to demold. Marked specimens are submerged vertically in water containers for curing as shown in Figure 15. Remove the specimens in water and cover with a damp cloth, then start strength testing, which is done for specimens that have been cured in water for 8h and 1 day.

Figure 15.specimens cured in water(left) inside 38 degrees container(right)

Prism is placed in a supporting roller horizontally and load applied vertically by means of loading roller on opposite side face of the prism and increasing it smoothly until it fractures into half. All prisms halves to be tested to be kept on a damp cloth until test commences. On the test machine, enter the specimen identification number. Test each prism half by placing it on the Test machine which has a Pressure indicating device that shows value at time of fracture of specimen as shown on Figure 16. This pressure would remain there until the next half is placed on the jig machine.

Figure 16. Specimens in damp cloth, crushed to get Compressive strength in MPa (left to right)

The machine already computes the compressive strength (Rc) of specimens as follows:

$$R_C = \frac{F_C}{1600} \quad \text{..... Eq 18}$$

Fc is the applied force to fracture the cube, 1600 is the 40 mm x 40 mm area of plate surface where the cube was placed for strength testing on Machine.

3.8 Thickening Time

500 g of cement is weighed and 136 g of water weighed, and mixed in a mixer as shown on Figure 17. Once the mixer machine is switched on at low speed, time of mixing is tracked with a stopwatch.

Figure 17. Measurement of water and cement using balance[Lafarge plant Laboratory]

Record start time as 'zero time', this will enable calculation of initial and final setting times. Mixer is stopped after 90s for 30s in order to scrap paste adhering on side walls so that mixing can give a uniform paste as shown on Figure 18. Restart mixer at low speed and run for 90s.

Figure 18. Mixing of paste in bowl[Lafarge Plant Laboratory]

The paste is then filled in a lightly oiled mold. Voids are removed in paste by gently using a ruler in a sawing motion to get a smooth upper surface. The mold filled with paste is then put on vicat apparatus in order to measure the paste consistency; Figure 19 illustrates this process.

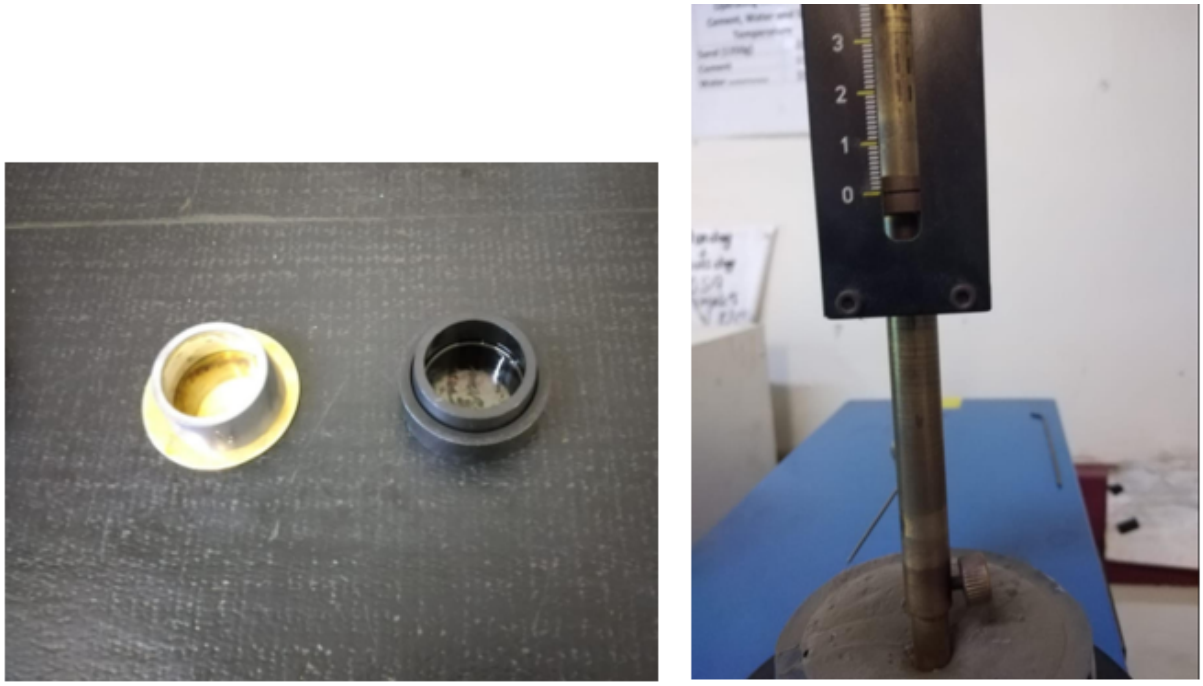

Figure 19.Thickening time molds and vicat Consistency test [Lafarge plant Laboratory]

The paste is positioned centrally under the plunger. The plunger is then lowered until in contact with cement paste, pause for 2 seconds to avoid forced acceleration of the moving parts then release the moving parts (this must be happening 4 minutes after zero time). Read and record scale after 30s of releasing the plunger. Repeat the test with different additive dosages, acceptable distance between plunger and base plate is 4-8mm.

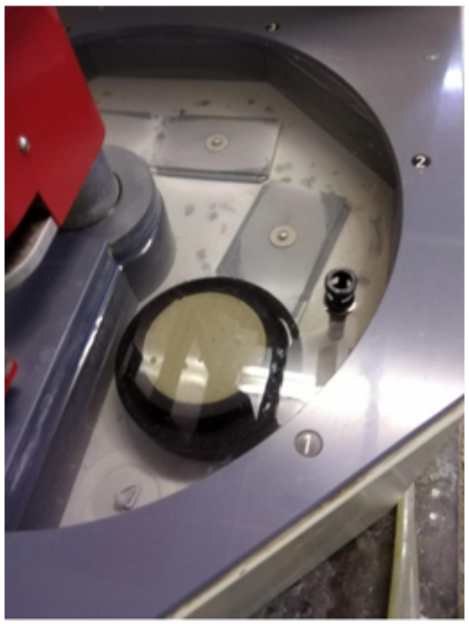

Figure 20. Automatic Vicat Needle Setting times Test [Lafarge plant Laboratory]

Figure 20 above shows the Toniset II automatic vicat needle setting times test; this is used in conjunction with computerized software that automatically calculates the setting times based on how deep the needle penetrates the cement paste. This above method is used mostly in construction cement, in oil well cement the method used is described below.

According to the API method, the slurry is prepared and put in a jug. Equipment used to test thickening times is a consistometer. The equipment consists of a cylinder jug that rotates and a fixed paddle. The jug is covered with a pressure container with liquid that can alter the operating temperature (Nelson & Dominique, 2006). A wellbore pressure of 103MPa is generated in all circumstances with different working temperatures of 25, 38, and 60 °C. As the consistometer maintains the slurry at a selected pressure and temperature, the rotating effect on stationary blade is measured and changed into a slurry consistency, in Bc (Bearden units). According to API standard 10, the thickening time is the time at which viscosity becomes 70 Bc (Nelson &

Dominique, 2006). Nevertheless, this method was not used due to unavailability of equipment and Covid restrictions.

3.9 Rheology

Rheological measurements are done using a rotational viscometer. Immediately after the slurry is mixed, it is then placed in a bowl for 20 minutes preconditioning at 150 rpm and 23, 38 and 60 °C (Nehdi, 2012). The container temperature must be initially at ambient temperature to avoid thermal shock to any admixtures in the slurry. The slurry is conditioned and then transferred to a heated viscometer cup as shown on Figure 21 below.

Figure 21. Slurry Testing using Fann 35A Viscometer [Lafarge plant Laboratory]

This cup is raised till the fluid level touches the line on the sleeve; this is done while the sleeve is rotating at its lowest speed (Nelson & Dominique, 2006). When the slurry temperature is observed, dial readings are recorded at different rotational speeds of 3, 6, 30, 60, 100, 200 and 300 rpm as shown in Figure 22.

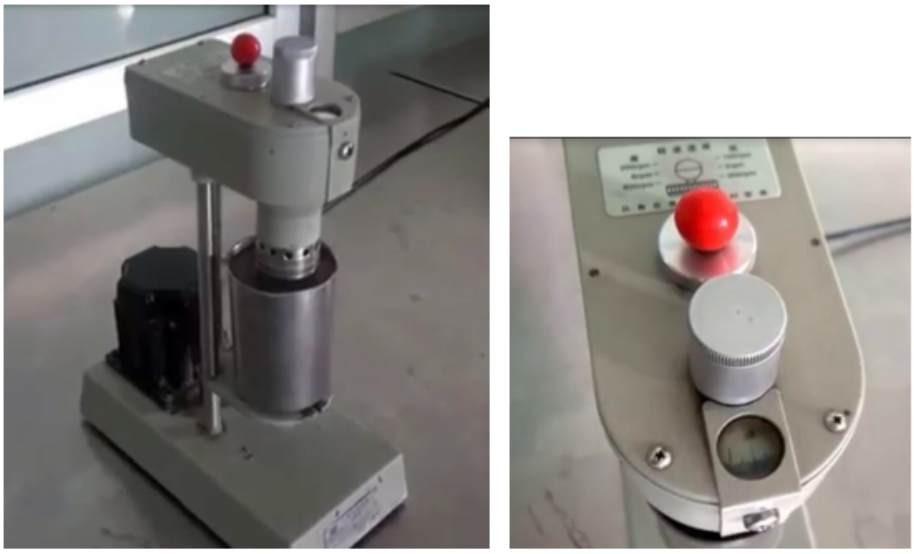

Figure 22. Cup raised (left) and dial readings observed (right) [Lafarge plant Laboratory]

Readings are initially taken in ascending order and then in descending order. The ramp-up and ramp down dial readings are averaged and then translated to shear rates and shear stresses by use of following equations (Nelson & Dominique, 2006):

$$shear\ rate = 1.705\ x\ rpm \quad \text{Eq 19}$$

$$shear\ stress = 0.5109\ x\ Pa \quad \text{Eq 20}$$

For Newtonian fluids, shear stress is directly proportional to the shear rate. The gradient or slope for this line is the dynamic viscosity of the liquid. Equation 21 below represents the Newtonian model (Lozhechnikova, 2011).

$$\tau = \mu \frac{dV}{dy} \quad \text{Eq 21}$$

Where:

μ is a viscosity of fluid,

τ is shear stress,

and dV/dy is a shear rate.

At given pressure and temperature Newtonian liquids exhibit constant velocity and constant viscosity. Fluids that are non-Newtonian typically do not follow same behavior as Newtonian fluids as shown on Figure 23 below:

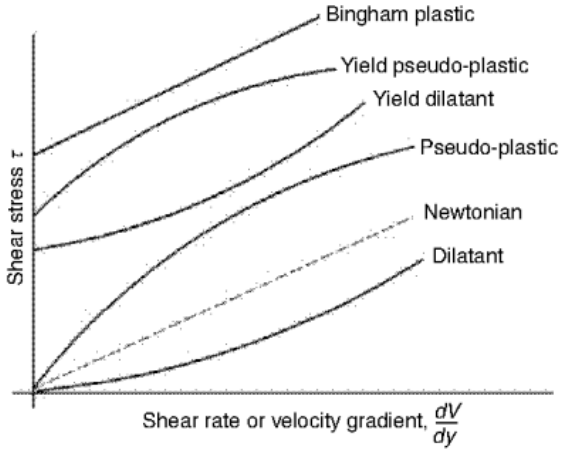

Figure 23. Newtonian and Non-Newtonian fluids flow behavior (Lozhechnikova, 2011)

Figure 23 above illustrates how Newtonian and Bingham plastic fluids have shear rate that is directly proportional to shear stress because of dynamic viscosity that is constant. Equation 22 represents the shear stress for the Bingham plastic model:

$$\tau = \tau 0 + \eta \frac{dV}{dy} \quad \text{Eq 22}$$

where τ0 is a yield stress,

η – rigidity coefficient,

Dilatant, Newtonian and Pseudoplastic fluids have lines passing through the origin and this means they do not need minimum shear stress to start movement i.e., zero shear stress at zero shear rate signifies that. Pseudoplastic and dilatant fluids have lines that are curved; therefore, viscosity changes are dependent on shear rate (Lozhechnikova, 2011). The Power-law model (or Ostwald-de-Waele) is used to define pseudoplastic and dilatant fluids as illustrated by following equation:

$$\tau = K[\frac{dV}{dy}]^{n} \quad \text{Eq 23}$$

Where:

n is power law exponent or flow index and

K is a power law coefficient or fluid consistency index

The flow index is used to measure deviation from Newtonian fluid behavior, where n=1. For pseudoplastic fluids, coefficient $n < 1$ and these fluids are said to be shear thinning as their viscosity decreases with shear rate. Dilatant fluids have n>1 and are shear thickening fluids with viscosity that increases due to shear rate. The fluid consistency index is usually high for higher viscosities (Lozhechnikova, 2011).

Yield pseudoplastic fluids (Herschel and Bulkley model) follow both the Bingham model and the power-law model as shown by Figure 24 below by (Lozhechnikova, 2011):

$$\tau = \tau_0 + K[\frac{dV}{dy}]^n \quad \text{..... Eq 24}$$

The shear-rate and shear-stress values are plotted to determine the best model that fits data between Power-law model and Bingham model. Other models are shown on Appendix A and will use the 2 models mentioned due to the fact that they are more commonly used than other models although they have defects reported as mentioned in Appendix A.

The cement slurry to be used for oil drilling needs to meet the American Petroleum Standards, as specified on Table 9:

Table 9. API Standard -Properties of class G cement (Nehdi, 2012; Nelson, 2006 & Rzepka, et al., 2016))

Chemical Component	**%**	**Physical Properties**	
SIO_2	21.6	Fineness 45 μm sieve	92.4% passing
Al_2O_3	3.3	Blaine	385 m^2/kg
Fe_2O_3	4.9	Thickening time at 52 ºC and 36.5 MPa	90-120 min at 100 Bc 15-30 min at 30 Bc
Total CaO	64.2	Compressive strength at 8h at 38 °C	2.1 MPa
MgO	1.1-6	Compressive strength at 8 h at 60 °C	10.3 MPa
SO_3	2.2-3	Maximum free water content	3.5 mL or (5.9% after 2 h)
Loss on ignition	0.6	Density	1900 kg/m^3(1400-2300 kg/m^3 accepted)
Insoluble residues	0.3-0.75		
Equivalent Alkali (Na_2O)	0.41-0.75		
C_3A	1-5		
C_3S	50-65		
C_2S	15-30		
C_4AF	12-15		

CHAPTER 4: RESULTS AND DISCUSSIONS

4.1 Density

Density measurements are performed after thorough mixing as some particles may precipitate in heterogeneous suspensions, if mixing is not done density results may be incorrect (Lozhechnikova, 2011). Cement slurries are categorized into three sections, normal density slurries (1750-1850kg/m^3), lightweight slurries (less than 1750kg/m^3) and heavy slurries (greater than 1900kg/m^3 (Kremieniewski, 2020). All the slurries prepared in this study were found to be lightweight slurries, with more Bentonite and Durapozz additives dosage at the same water to cement ratio the density decreases.

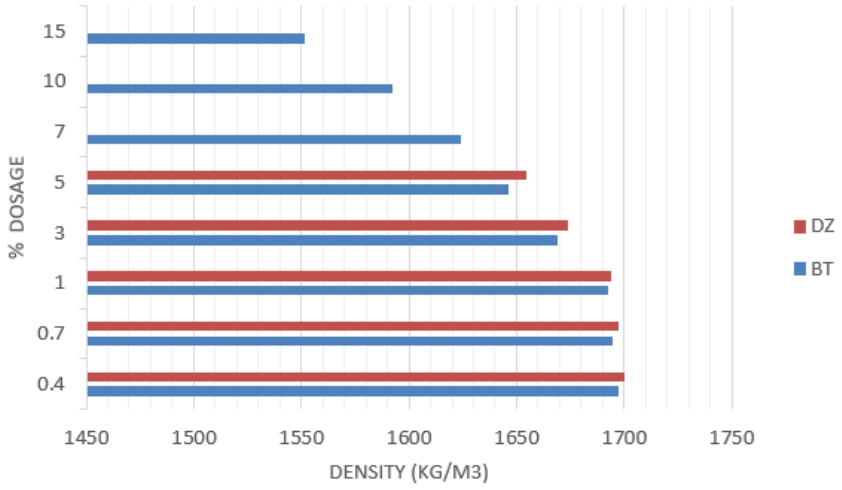

Figure 24. Density of slurries

BT absorbs high water content and therefore decreases the density of the slurry more than DZ by increasing its volume. The density of slurry depends on solid particle density, liquid density as well as the percent dosage of the solid. Figure 24 results show that DZ is denser than BT; therefore, DZ slurries are denser compared to BT slurries. Density is also a function of particle size distribution. DZ has a wide range of coarse and fine particles compared to BT, which has a narrow particle size distribution; this makes DZ to have better packing ability than BT (Lozhechnikova, 2011). With better packing ability, less porosity is an advantage as it limits

exposure to attack by sea water and other harsh conditions, which in turn makes the slurry to be more durable.

The API test methods study the bulk properties of the cement and do not take into consideration the differences in surface area of the individual phases. In the presence of additives these differences can have a significant effect on the hydration properties and morphological characteristics of the phases produced and ultimately impact on cement performance and may lead to a poor cementing job. Additive reactions with cement phases differ depending on the type of additive, variations in additive chemistry, and can be enhanced by synergistic effects between the additives (Lota, 2013).

Most lightweight slurries are used when sealing annulus in rock profiles that are penetrable. This limits the seepage of cement into low-pressure zones, thereby reducing hydrostatic pressure during cementing. Reduction of drilling mud hydrostatic pressure finally leads to a breakdown of a wellbore and more difficulties. Consequently, use of low-density slurries is crucial in sealing casing string columns embedded in loose formation strata. Therefore, density of slurry is selected based on environmental and mechanical conditions resulting from physical erection and distance of the well (Kremieniewski, 2020).

The lowest density that can be achieved by using water-extending additives, while the cement has satisfactory properties, is 1498 kg/m^3. Ultra-lightweight cement slurry could decrease the compressive strength of the cement slurry.

4.2 Compressive Strength

4.2.1 Effect of curing time

Adequate w/c ratio allows CS to never decrease over time. Less water means the slurry becomes very porous which leads to reduced CS, more water causes CS to be low. At lower water to cement ratios compressive strength may be slightly higher but the hydraulic bonding of cement is very low, and viscosity of cement increases.

The curing days chosen are based on standardization and same testing conditions for the construction industry. This is also important for planning of construction works ahead so that there is no waiting until concrete gains its full strength. Compressive strength is not analyzed between 7 to 28 days due to the fact that access to the lab during Covid-19 was on a bi-weekly rotational basis, which contributed to the analysis of samples at 14th day of curing a challenge. According to the construction industry, by the 14th day the strength of the cube will have gained about 90% of the expected strength and on the 28th day about 99% of expected strength is gained. For CEM I sulfate resistant cement strength is expected to be above 52.5Mpa by 28th day of curing. For the analysis conducted by the 7th day of curing, cement strength was above 80% of expected strength. Beyond 28 days strength may continue to increase but at a very slower rate.

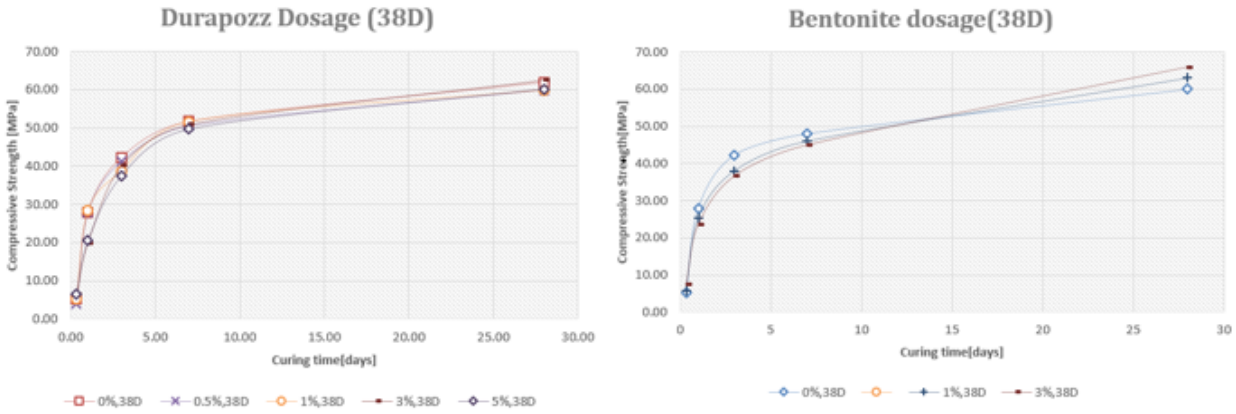

Figure 25. i. Durapozz and ii. Bentonite Compressive Strength over time

Figure 25 shows that with prolonged curing time compressive strength increases, however for much longer periods of time strength may cease to increase as hydration is completed. CSH gel formed during hydration reactions allows CS to rise rapidly on early curing and slows down with time and finally constant when hydration is finished. Rate of increase in compressive strength faster at lower DZ dosage.

Initially when hydration progresses lightweight slurries have lower compressive strength, after 24h the hydration rate improves and compressive strength of greater than 10 MPa can be observed. Both BT and DZ seem to have a decrease in early compressive strength when additive dosage is increased but this decrease is still within acceptable limits (8 h curing >2.1 MPa).

4.2.2 Effect of temperature

Figure 26 below shows the BT and DZ slurries behavior when exposed at 23 and 38°C. Bentonite and DZ gain strength at higher temperature. The higher the temperature the higher the compressive strength due to activation of mineral-to-mineral reactions, as temperature is further increased compressive strength starts to decrease due to drying and weakened structure of the cement. At higher dosages, high temperature affects early strength. With Bentonite gelation at 3% substitution, it was noticed that more water is needed as bentonite expands when wet, that is why it is mostly used as a sealant. At lower dosages, high temperature may affect late strength. Early strength not affected by temperature at lower dosages for DZ slurries. Disadvantages of bentonite slurry are their low resistance to much high temperatures and corrosive water (Larki, et al., 2019).

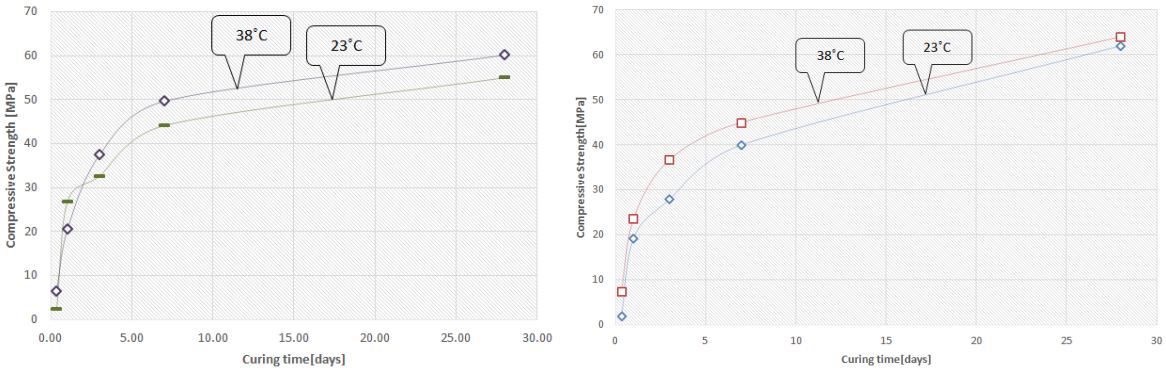

Figure 26.temperature effect on 5% durapozz (left) and 3%bentonite (right)

Increase in temperature affects the hydration process by generally decreasing the setting times of cement. The CSH gel formed during hydration largely depends on temperature for it to be steady. CSH gel remains unchanged up to temperatures of about 40 °C (Munjal, et al., 2019). From 40°C to 110°C, the structure of the gel starts to change. Above 110°C, CSH gel will have completely changed and this causes increased permeability and reduced compressive strength of cement slurry. At this stage strength, retrogression occurs and challenges are encountered in an oil wellbore. Addition of silica-based material such as silica fumes and silica flour will help prevent strength retrogression by lowering the lime to silica ratio in the CSH gel to about one (Munjal, et al., 2019).

When silica is added $C_5S_6H_5$ forms and conserves high strength and low porousness at 110°C. At above 150°C $C_5S_6H_5$ is changed to C_6S_6H. With high aluminum, $C_5S_6H_5$ can remain in its phase up to temperatures of 250°C. Above 250°C $C_7S_{12}H_3$ emerges and this remains steady up to temperatures of 350 °C if silica quartz is added or sometimes 390°C when silica acid is added.

$$C_3S_2H_4 + 4S + 2C + H \xrightarrow{110^\circ C} C_5S_6H_5$$

……..…Eq 25

$$C_5S_6H_5 + C \underset{400^\circ C}{\overset{150^\circ C}{\rightleftharpoons}} C_6S_6H + 4H$$

.....Eq 26

$$C_6S_6H + C + 6S + 2H \underset{400^\circ C}{\overset{250^\circ C}{\rightleftharpoons}} C_7S_{12}H_3$$

……Eq 27

At about 400°C $C_7S_{12}H_3$ and C_6S_6H starts to dehydrate, destroying the set cement. Therefore, temperature and pressure changes the CSH gel phases by altering C/S ratio as well as altering of silica fume particles (Munjal, et al., 2019).

Durapozz has low pozzolanic reactivity and therefore needs to be activated by grinding so that it can be widely used. Compared to other suggested lightweight slurries, the developed slurry shows higher early compressive strength. Another advantage from the chemical properties of durapozz is that they decrease or even eradicate the harmful reaction between certain reactive aggregates and the alkaline products of cement hydration as explained by use of silica fumes.

4.3 Thickening Time

With more dosage DZ thickening time decreases and BT thickening time continues to increase, this is due to that DZ is coarser than bentonite and therefore particle-to-particle reactions are

slower and hydration becomes slow. Acceptable thickening time is 90-120 min but can go up to 5 h, depending on total calculated pumping time of slurry. In general pumping time should be less or equal to thickening time to avoid any blockages. Both BT and DZ can be used at downhole conditions provided bentonite w/c ratio is improved for better flow ability and viscosity.

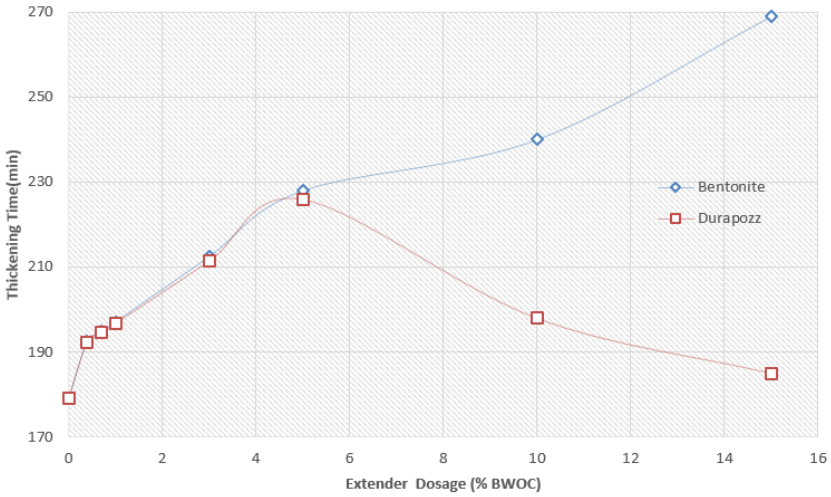

Figure 27. Thickening time of additives

Addition of more BT into the slurry decreases its flowability at low temperatures. This reaction needs to be investigated at much higher temperatures and increased w/c ratio to see how thickening time behaves. Increase in temperature generally decreases thickening time (TT), and therefore cement slurry sets quicker (Larki, et al., 2019). Figure 27 above shows that DZ can be used in place of BT at dosage up to 5%. Using DZ at high dose may cause blockage in the annular of the wellbore as shown by thickening time decreasing.

Correlation of BZ TT and DZ TT (Figure 28) shows that the thickening times are same, therefore BT can be substituted by DZ only at dosages below 5%, and this will save costs, as BT is more expensive than DZ.

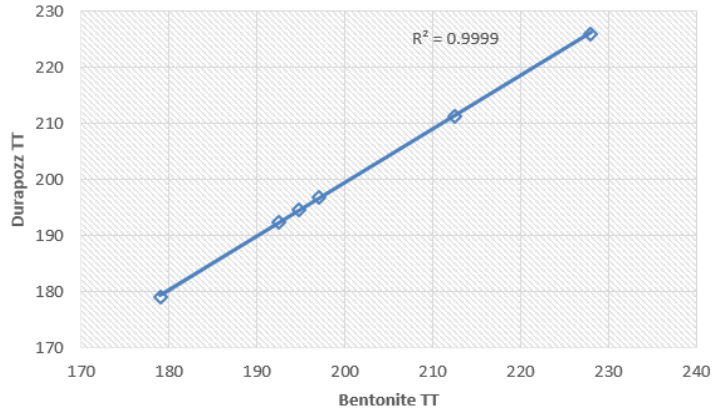

Figure 28. Correlation

Precise time required for the procedure is essential; this includes mixing time of slurry, mud and spacer displacement time, time of releasing plug as well as safety time. These times greatly influence thickening time of the slurry in downhole conditions.

When well temperature increases, the faster the cement slurry sets or the lower the thickening time. That increase in retarder concentration increases the thickening time of the cement slurry (Anaele & Otaraku, 2020). Therefore, DZ can work as a retarder and accelerator in various cases as thickening time increases and then decreases with dosage. The developed slurries contain less water and their thickening times are comparable provided they are mixed with retarders and accelerators in order to have good flowability. Short thickening times can have disastrous consequences due to loss of slurry circulation in the Well. Slurry circulation problem occurs if the pumping time is longer than the actual slurry thickening time.

4.4 Rheology

Average pressure at different dial readings was determined by ramping up and ramping as shown in Table 10. This pressure was used to calculate shear stress using Equation 19 as stipulated in Chapter 3.2.The shear rate was calculated using Equation 20.

Table 10. Pressure obtained from different dial readings

0% Durapozz Slurry				
Dial Reading(rpm)	Ramp up (Pa)	Ramp down (Pa)	Reading Ratio	Average Reading (Pa)
3.00	30.00	32.00	0.94	31.00
6.00	36.00	38.00	0.95	37.00
100.00	49.00	53.00	0.92	51.00
200.00	62.00	66.00	0.94	64.00
300.00	79.00	84.00	0.94	81.50

Table 11. Shear rate and stress

Shear Rate, ў(1/s)	Shear Stress, τ(Pa)
5.12	15.84
10.23	18.90
170.50	26.06
341.00	32.70
511.50	41.64

Table 12. Shear stress (in Pascals) from Models

τ,power	τ,bingham	error-power	error-bingham
15.90	17.40	0.4%	9.9%
18.02	17.64	-4.7%	-6.7%
29.93	25.25	14.9%	-3.1%
33.91	33.35	3.7%	2.0%
36.48	41.45	-12.4%	-0.4%
corr coeff-power	corr coeff bingham		
0.9505	0.9941		

Shear rate was plotted against shear stress in order to find the rheological model that best suits the slurry as illustrated by Table 11 and 12. The results of different dosage of DZ slurries are found Figure 29 and 30 below:

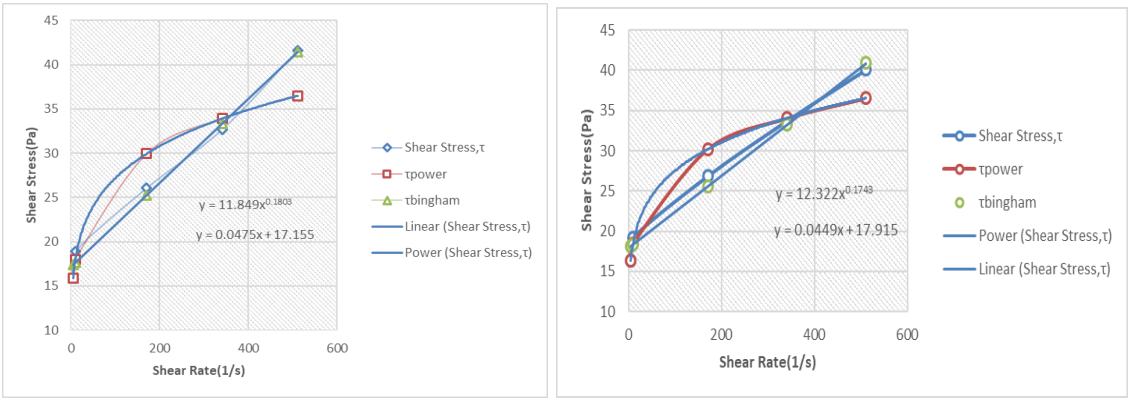

Figure 29: 0% Durapozz(left),1% Durapozz (right)

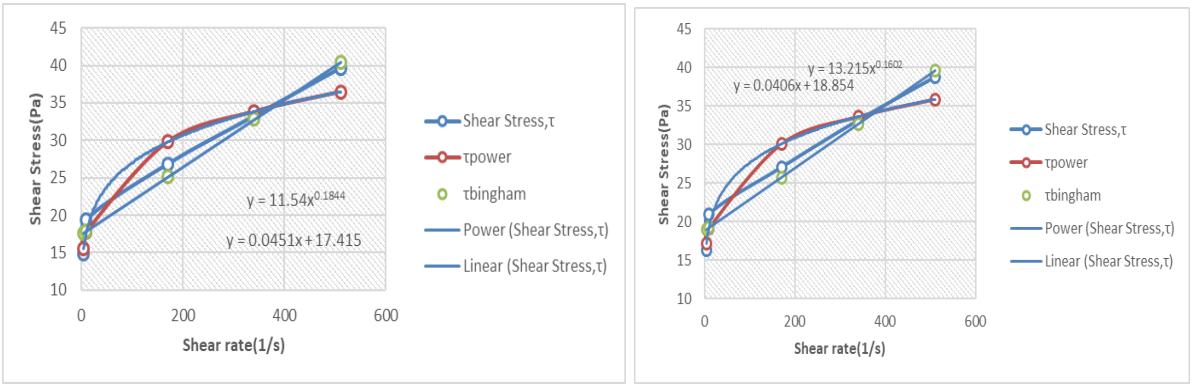

Figure 30: 3% Durapozz(left) & 5% Durapozz (right)

The Bingham plastic model was determined to be best fit for all the Durapozz slurries and not the power model as shown by higher correlation coefficient. Table 13 below summarizes the constants for the two models as determined from Figures above. Bingham fluids sustain a firm structure and do not move if the shear stress is less than yield stress. High viscosity slurry affects pumping operation.

Table 13. Power and Bingham models constants

Dosage	n	K (Pa-s^n)	τy(Pa)	μp(mPa-s)
0% DZ	0.1803	11.849	17.155	0.0475
1% DZ	0.1743	12.322	17.915	0.0449
3% DZ	0.1844	11.54	17.415	0.0451
5% DZ	0.1602	13.215	18.854	0.0406

Because n is less than 1, the slurries prepared are all shear thinning according to power model i.e., non-Newtonian fluid viscosity decreases under strain; which means the slurries would be able to flow in the annulus of wellbore. Plastic viscosity (μp) is very low and this permits the rate of drilling to be quicker, especially if there is less concentration of solids. Yield point (τy) or threshold stress, must be high to move cuttings out of the hole but not too high and generate extreme pump pressure when beginning mud flow.

From the time the slurry is mixed with water to when the slurry sets, viscosity will be increasing until the slurry is too thick and does not move. Hence, it is crucial to put the cement within a certain defined time after mixing; else, disastrous loss of the well might take place. Low fineness and low C3A can help decrease viscosity. The smaller the size of the particles, the better the chance that fluid will demonstrate a non-Newtonian characteristic. For slurries with the equal solids' concentration, the slurry with fine particles will have higher consistency; in this case, BT would have better consistency than Durapozz.

DZ has better packing density than BT due to the fact that it has larger particle size distribution than BT. As DZ concentration of solids increases, the level of non-Newtonian behavior increases.it is expected that while concentration increases apparent viscosity also increases proportionally with density, until a critical concentration will be reached. For lightweight slurries this is not the case as density decreases therefore viscosity also decreases with more DZ dosage.

It was also noted that increasing shear rate caused the slurry to exhibit time dependent reduction of apparent viscosity and also when slurry is left untouched for some time it reverts back to

original viscosity. The apparent viscosity of DZ slurries shows slight reduction with the prolongation of shearing at fixed rate, this characteristic shows thixotropic fluid. (Lozhechnikova, 2011). This behavior shows that apparent viscosity relies on both rate of shear as well as time to which the slurry is exposed to shearing. When the slurry is allowed to settle after long periods and then sheared, apparent viscosity becomes less than original viscosity due to that interior structure of the slurry particles is broken. The rate of change of viscosity with time will eventually be zero because of the decrease in the amount of structural bonds that can be broken down. Also, when part of the bonds is destroyed, new bonds can re-form at a faster rate. Therefore, the dynamic equilibrium is reached when there is balance between the rates of creation and destruction of links.

Turbulent flow is preferred during mud removal due to that if its laminar flow particles accumulate near the wellbore wall and velocity becomes zero. This makes displacement very difficult. Pumping turbulent spacer fluid to displace mud ensures current move surfactants throughout the wellbore allowing removal of static mud layer on wellbore wall. For cement pumping, laminar would be preferred due to high friction pressure losses in narrow sizes and tight holes, but in reality, turbulent flow is what happens. High pressure would fracture the formation causing loss in circulation.

4.5 Free fluid

Too much turbulence in cement slurries is also not ideal as this would cause some formation to break due to high pressure exerted, this would consequently lead to leak of fluid to and from the formation thereby weakening the structure of the cement slurry. To prevent formation damage free fluid is tested to have a clear indication of how much fluid is left on the cement paste after it sets.

A factorial design (FD) technique was used to determine the free fluid content (FFC) using results obtained from experimental data. Equation 25 below illustrates how the number of experimental runs (N) is determined:

$N = F^K$ ……..……...……Eq 28

Where:

F is number of factors involved

K is the level number

Since 2 additives are used, F will be equal to 2 and K is usually set at 2, therefore N will be equal to 4. Using Equation 25, 4 tests were performed to include all the probable combinations of factors. FFC of the cement slurry is taken as the response variable in the FD. The comprehensive designs of the experimental runs are shown in Table 14.

Table 14. Factorial Design number of experiments

Experiment number	**Factors (additives at 5% dosage)**	
	DZ	**BT**
1	✓	✓
2	✓	X
3	X	✓
4	X	X

In Table 14, the (✓) symbol represents the inclusion of the additive at 5% dosage. The (X) symbol represents the exclusion of BT or DZ. The nominated dosage of additives is based on results obtained from thickening times, DZ can be added up to 5%.

Based on Table 14, cement slurries are formulated and organized as per standard procedures. Then the FFC of each formulation is determined using the described technique. The outcomes of the four tests are shown in Table 15below:

Table 15. Experimental results used to develop FD equation

Experiment number	Durapozz	Bentonite	FFC%
1	✓	✓	1.52
2	✓	X	3.58
3	X	✓	3.21
4	X	X	2.72

Including all four potential combinations of factors, the response variable is determined by experimental technique. The results of experiments shown in Table 15 are used to determine a mathematical model, which contains the key effects of each factor and the interaction effects. In the determined model, there are two main effects and 1 two-factor interaction (Moradi & Nikolaev, 2017). The model is illustrated below:

$$\%FFC = cte + \alpha_1 A_1 + \alpha_2 A_2 + \alpha_3 A_1 A_2 \quad \text{.....Eq 29}$$

The coefficients of equation 25 are determined using data obtained experimentally as well as using multiple linear regression techniques. A_1 and A_2 are additives 1 and 2, which represent Durapozz (DZ) and Bentonite (BT) respectively. The mathematical model, which can be used to calculate the FFC of the slurry, is defined by equation 30 below:

$$\%FFC = 2.72 + 0.172A_1 + 0.098A_2 - 0.048A_1A_2 \quad \text{..... Eq 30}$$

By using this equation can determine FFC at different durapozz and bentonite dosages, results of this are shown in Figure 31.

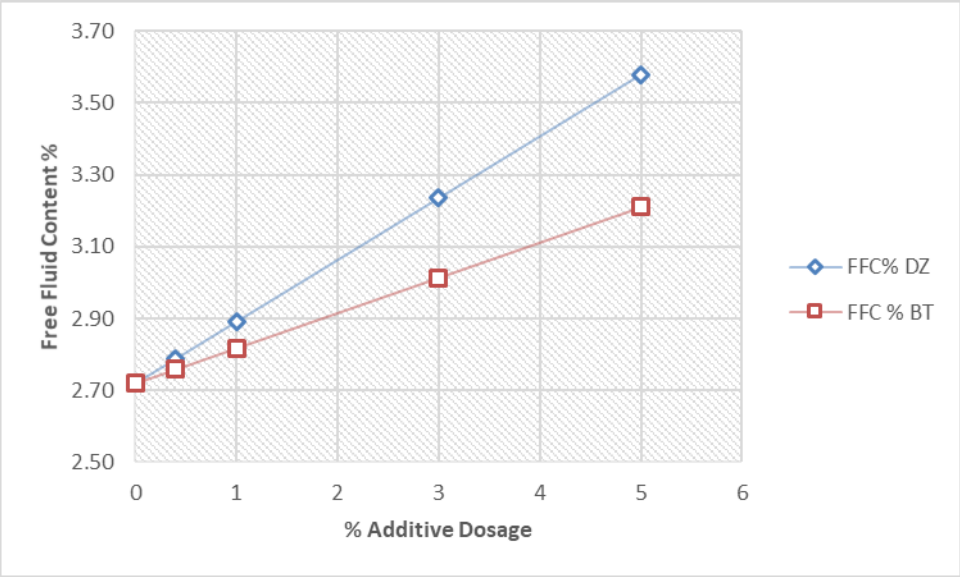

Figure 31. FFC by Factorial Design

Because slurries prepared are lightweight and contain less water, lower free fluid content was obtained. Low free fluid content gives an advantage of inhibiting gas migration after cementing and gives better wellbore annulus sealing. However, lightweight slurries with low free fluid content have a risk of lower mechanical strength. To lower the rate of compressive strength, decrease strengthening agents are to be added to the slurry. High free fluid (and field bleed) leads to poor bonding between the casing and the formation. The loss of water to the formation will result in a dehydrated cement slurry, which is friable, and with low compressive strength.

CHAPTER 5: CEMENT DESIGN FRAMEWORK

5.1 Raw Materials Design

The cement quality largely depends on the raw materials used to make the clinker; hence, optimization of these raw materials plays an important role economically. Table 16 shows the inputs or manipulated variables that would give outputs or quality parameters to look out for during the optimization process. The raw materials are selected based on their chemical composition and compatibility with the main raw material (limestone) as well as fuel used.

Table 16. Inputs and Outputs of Raw mix Design

Inputs	Outputs
Raw Materials chemical composition	Clinker chemical composition
Ash fuel chemical composition	Burning temperature
Raw mix dosage(tph)	Sulfur alkali ratio
Fuel dosage(tph)	Kiln coating tendency
Raw mix conversion factor to clinker	

One of the outputs to monitor is the coating tendency inside the kiln. Figure 32 shows that if SR and AR are within circulated area then the coating is good, otherwise if AR and SR are outside of the circle then one of the four disastrous incidents may occur such as refractory lining failure inside the kiln or difficulty in burning the material inside the kiln.

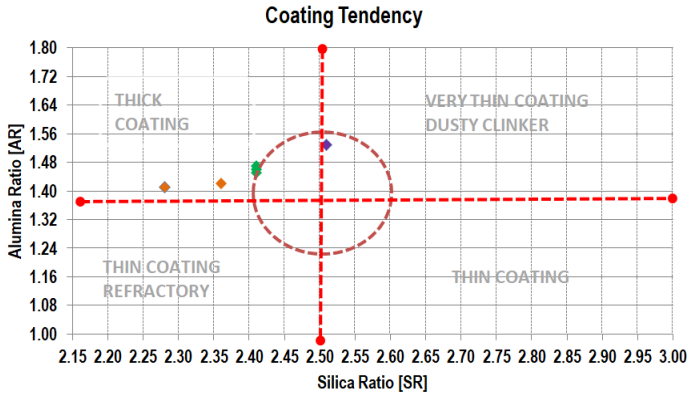

Figure 32. Kiln Coating Tendency

The main burning effectiveness indicators are the remaining lime content (free CaO) when the reaction has completed as well as the lime saturation factor (LSF). If there is any deviation in clinker quality, LSF is corrected by altering SR by changing silica containing raw material proportion, SR corrected by AR. Low SR restricts the conversion of C2S to C3S, making C2S to be high and consequently higher liquid phase content.

The clinker phases are also monitored as they have different roles in cement quality, these are defined below:

1. C3S responsible for short-term strength of cement.
2. C2S signifies long term strength.
3. C3A is important in hydration of cement.
4. C4AF gives cement its color

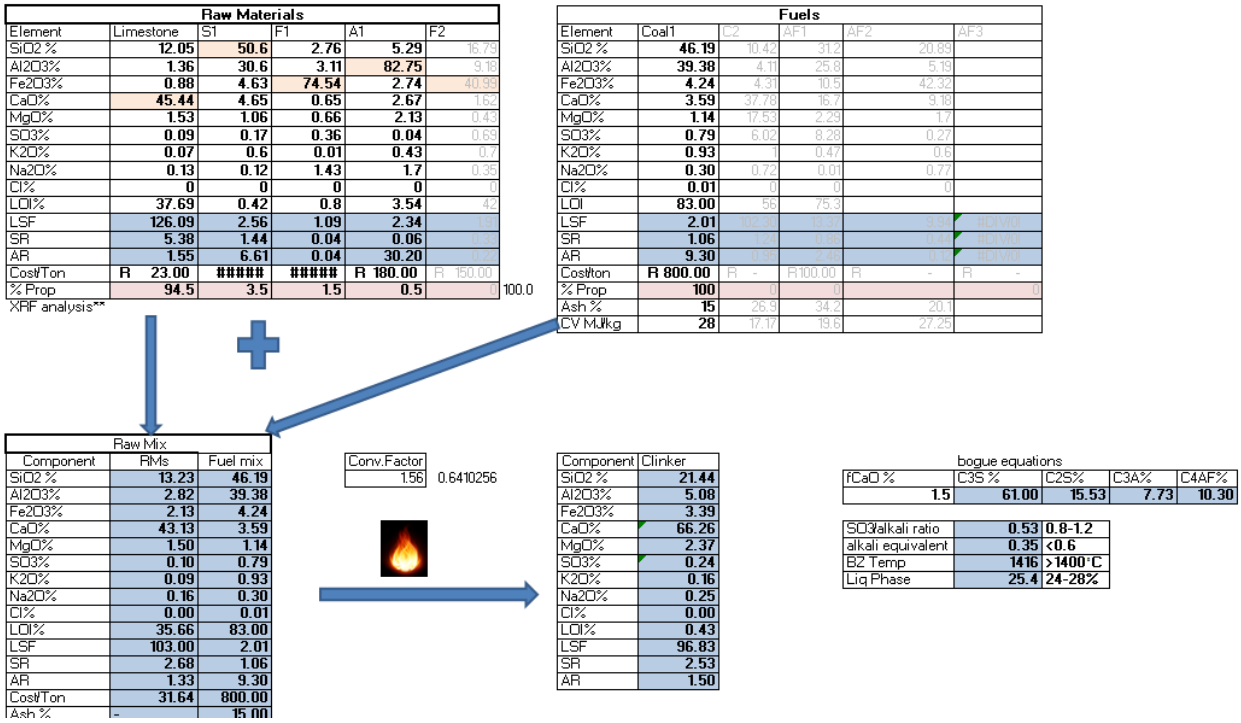

Figure 33. Resultant Clinker Designed

Figure 33 shows the quality of developed clinker as obtained from raw materials and fuel proportions as well as bogue calculations. Designing cement slurry that would be suitable for wellbore conditions begins in how the cement is produced, and this in turn is greatly influenced by the selection of raw materials for the cement manufacturing process. Maintaining the ratio of fuel to raw mix to get the same clinker quality is key to ensure that the clinker produced is not overburnt or under burnt. Increased coal ash percent lowers calorific value of fuel, drops burning temperature, and lowers C3S.

5.2 Cement Design

When clinker is made it is then sent to a grinding station for milling to make cement. During milling gypsum is added to control setting times, in gypsum SO3 is significant in ensuring cement hydration progresses well. The fineness of cement also affects the hydration.

5.2.1 SO3 and fineness effect on cement

It is very important to understand the reactions that take place during the hydration of Portland cement in order to assess the effect of the SO3 content of the cement. Practical experience has shown that cements low in C3A, but high in C4AF are much more resistant to sulfate attack (Hanhan A A,2004).

The fineness of cement has an important bearing on the rate of hydration and hence on the rate of gain of strength and also on the rate of evolution of heat. Finer cement offers a greater surface area for hydration and hence faster the development of strength. Fineness is usually determined by sieving or by determination of specific surface expressed as cm^2/gm or m^2/kg.

Component	Clinker	Gypsum	Cement
SiO2 %	21.44	2.9	20.88
Al2O3%	5.08	0.13	4.93
Fe2O3%	3.39	0.49	3.30
CaO%	66.26	32.26	65.24
MgO%	2.37	0	2.29
SO3%	0.24	72.25	2.40
K2O%	0.16	0	0.15
Na2O%	0.25	0	0.24
Cl%	0.00	0	0.00
Prop %	97	3	100
cost/ton	800		1600
moisture		21.24	0
density kg/m3	1700		2800

Figure 34. Resultant Cement Designed

Figure 34 shows the chemical composition of the cement developed by using 97% of clinker and 3% of gypsum, thereby creating a Sulfur resistant cement.

5.3 Cement Slurry Design

Figure 35 below shows the process of preparation for cementing. It is important to note that dry cement is mixed with dry solid additives and homogenized or blended before water addition. The liquid additives are added with water before mixing with solid mixture in order to obtain a homogeneous liquid mix. Once this is done, the liquid and solids are mixed in the cement mixer. Thereafter they are ready to be pumped.

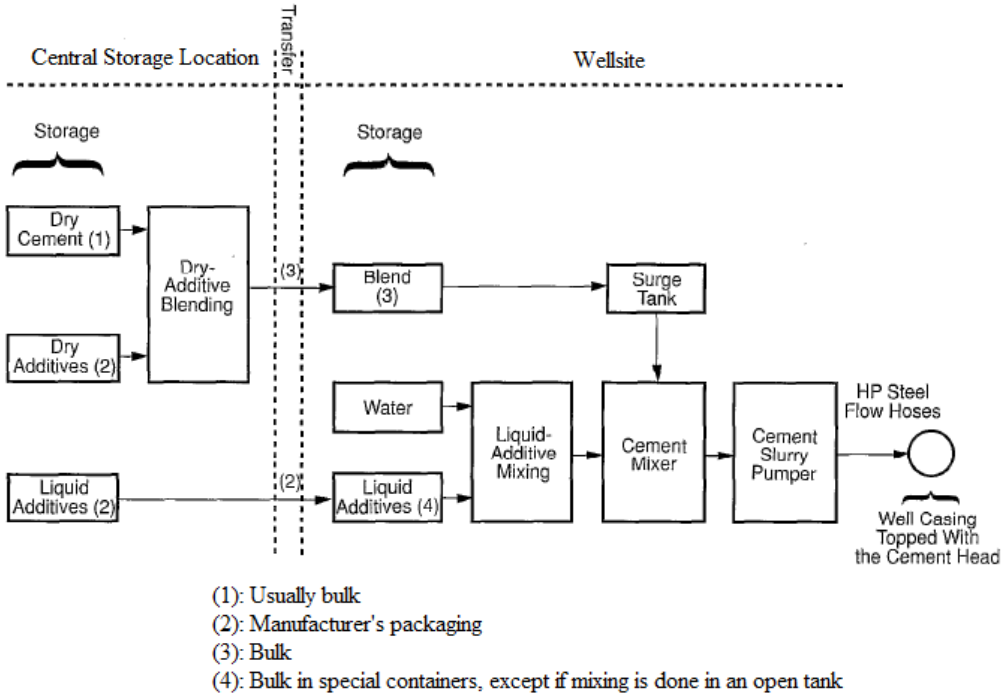

Figure 35. Process flow schematic for preparation of cementing (Bett, 2010)

Figure 36 below shows the resultant slurries from mixtures of cement with BT and cement with DZ. It is evident that with BT, it costs R5000 per ton, this is more expensive than DZ which only costs R186 per ton. Because Bentonite is more expensive than the cement, more dosage of bentonite means higher cost. With lower cost of durapozz, higher doses would save more cost as the cement required will be much less. Figure 37 shows the design of slurry from limestone and other raw materials and summarizes the process from quality of limestone mined to best cost effective cement slurry ,in this case Durapozz was more cost effective.

Component	Cement	Bentonite	Durapozz
SiO2 %	20.47	55.69	50.6
Al2O3%	4.62	18.41	30.6
Fe2O3%	3.28	6.35	4.63
CaO%	65.12	2.87	4.65
MgO%	2.42	3.54	1.06
SO3%	2.60	0.00	0.00
K2O%	0.15	0.58	0.60
Na2O%	0.24	3.24	0.12
Cl%	0.00	0.00	0.00
cost/t	1600.00	5000	186
moisture		8_15	11.3
density kg/m3	2800.00	1000	1100

% Bentonite	0.4	0.7	1	3	5	7	10	14
Slurry no.	1	2	3	4	5	6	7	8
SiO2 %	21.02	21.12	21.23	21.92	22.62	23.32	24.36	25.75
Al2O3%	4.98	5.03	5.07	5.34	5.60	5.87	6.28	6.82
Fe2O3%	3.31	3.32	3.33	3.39	3.45	3.52	3.61	3.73
CaO%	64.99	64.81	64.62	63.37	62.12	60.88	59.00	56.51
MgO%	2.30	2.30	2.31	2.33	2.36	2.38	2.42	2.47
SO3%	2.39	2.39	2.38	2.33	2.28	2.23	2.16	2.07
K2O%	0.15	0.15	0.16	0.16	0.17	0.18	0.19	0.21
Na2O%	0.25	0.26	0.27	0.33	0.39	0.45	0.54	0.66
Cl%	0.00	0.00	0.00	0.00	0.00	0.00	0.00	0.00
cost R/ton	R 1 613.60	R 1 623.80	R 1 634.00	R 1 702.00	R 1 770.00	R 1 838.00	R 1 940.00	R 2 076.00

% Durapozz	0.40	0.70	1.00	3.00	5.00
Slurry no.	1	2	3	4	5
SiO2 %	21.00	21.09	21.18	21.77	22.37
Al2O3%	5.03	5.11	5.19	5.70	6.21
Fe2O3%	3.31	3.31	3.32	3.34	3.37
CaO%	65.00	64.82	64.64	63.42	62.21
MgO%	2.29	2.29	2.28	2.26	2.23
SO3%	2.39	2.39	2.38	2.33	2.28
K2O%	0.15	0.15	0.16	0.16	0.17
Na2O%	0.24	0.24	0.24	0.24	0.24
Cl%	0.00	0.00	0.00	0.00	0.00
cost R/ton	R 1 594.34	R 1 590.10	R 1 585.86	R 1 557.58	R 1 529.30

Figure 36. Resultant Slurries Designed

With more additive dosage, the density of slurry becomes lower. For durapozz ,the lower the density the lower the cost of the slurry and for bentonite the lower the density, the higher the cost of slurry as shown in Figure 37. Lightweight slurries are used in areas with low formation pressure; it would be suitable on the surface of a wellbore up to 1830 m.

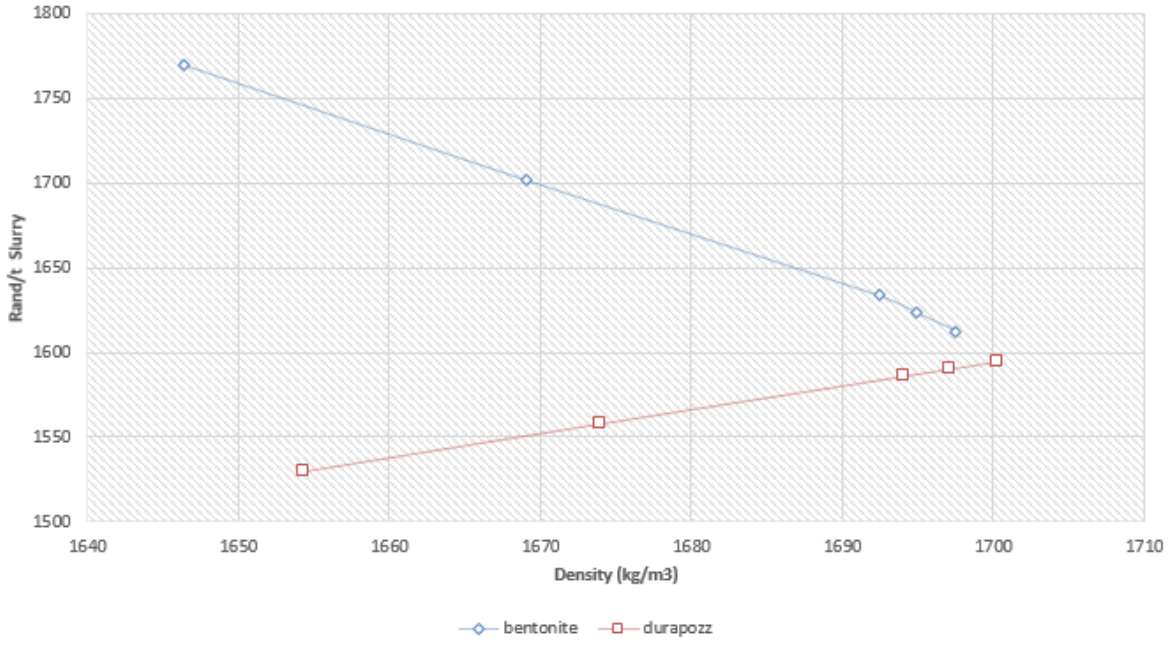

Figure 37. Density effect on cost of Additive

Figure 38 shows the design of slurry from limestone and other raw materials and summarizes the process from quality of limestone mined to best cost-effective cement slurry, in this case Durapozz was more cost effective.

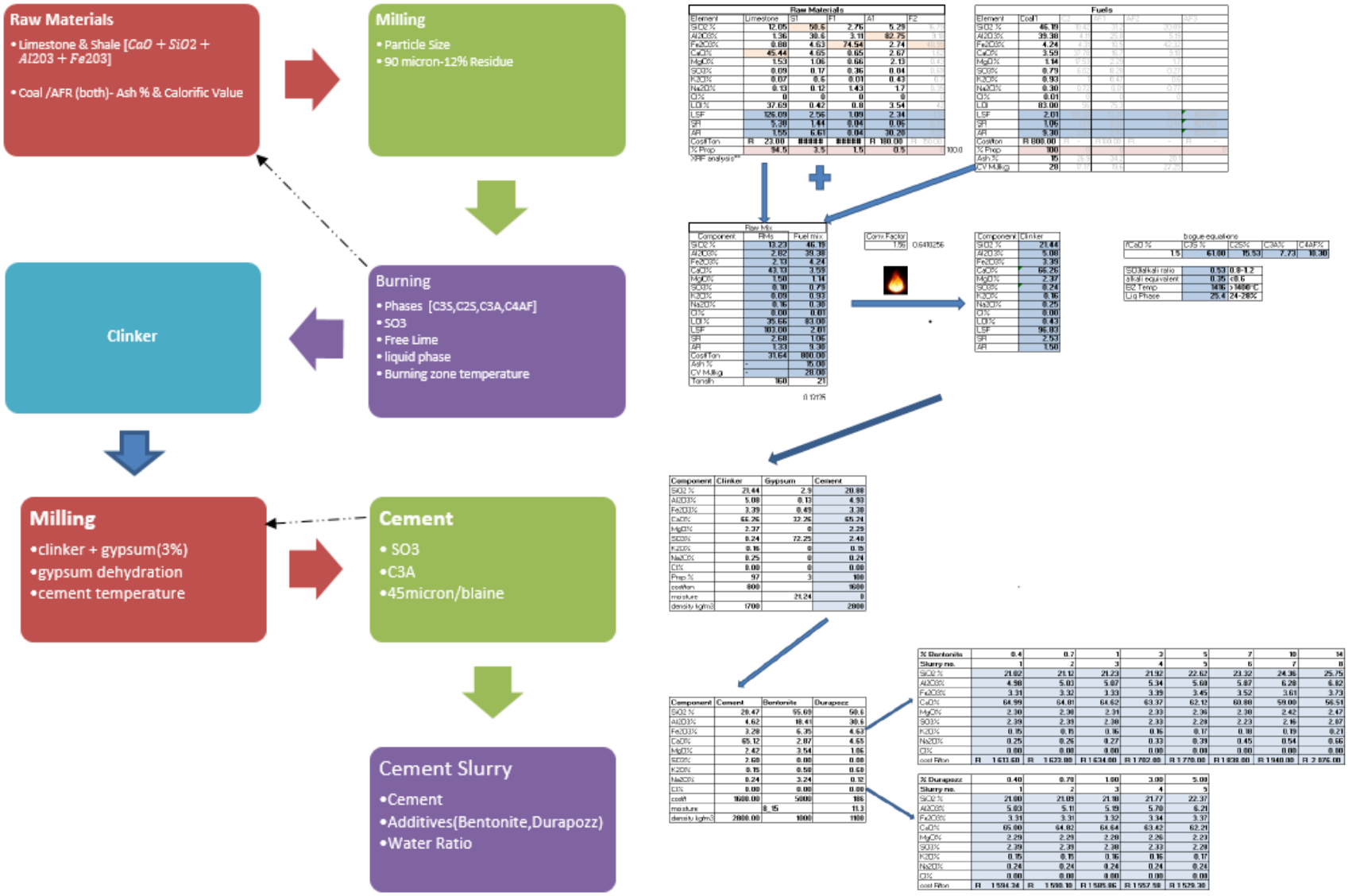

Figure 38: Cement Design Framework

5.4 Summary of Results

Table17. Benchmark of Results with API Requirements

	API Limit		1% DZ	3% DZ	5% DZ		1%BT	3% BT	5%BT
SiO2 %	21.6		21.18	21.77	22.37		21.23	21.92	22.62
Al2O3 %	3.3		5.19	5.70	6.21		5.07	5.34	5.60
Fe2O3 %	4.9		3.32	3.34	3.37		3.33	3.39	3.45
CaO %	64		64.64	63.42	62.21		64.62	63.37	62.12
MgO %	6		2.28	2.26	2.23		2.31	2.33	2.36
SO3 %	3		2.38	2.33	2.28		2.38	2.33	2.28
K2O %	-		0.16	0.16	0.17		0.16	0.16	0.17
Na2O %	-		0.24	0.24	0.24		0.27	0.33	0.39
Na2O Eq max.	0.75		0.34	0.35	0.35		0.37	0.44	0.50
LOI max.	3		0.10	0.11	0.12		0.18	0.35	0.52
C3S %	48-65		55.74	42.94	30.14		56.07	43.94	31.81
C3A % max.	8		8.1	9.5	10.8		7.8	8.4	9.0
C4AF % max.	15		10.08	10.16	10.24		10.13	10.32	10.50
C4AF+2C3A max.	24		26.37	29.08	31.79		25.71	27.12	28.53
Blaine m2/kg	385		436	440	444		439	444	449
Free fluid % max.	5.9		-	-	3.58		-	-	3.21
Mpa strength (38 D)8hrs min.	2.1		5.2	6.4	6.5		5.8	7.4	-
Thickening times (min)	90-120		197	211	226		197	212	228

Table 17 above shows that the selected additive alone can be used only at low dosages (DZ less than 1% and BT less than 3%), above these dosages results deviate much more from the API limit. Investigations to be further done by using these additives together with other additives that would be suitable to correct the parameters that did not meet the API limit.

The rheology results were inputted in PVI drilling software (Appendix C1) and it showed that flow index and plastic viscosity were the same, however fluid consistency index and yield stress showed slight differences as shown by low error in Table 18.

Table18. Comparison with Drilling Software result

DZ dosage	K, Calculated	K, Software	K, error	τy, Calculated	τy, Software	τy, error
0%	11.849	11.245	-5.4%	17.155	16.080	-6.7%
1%	12.322	11.689	-5.4%	17.915	16.790	-6.7%
3%	11.540	10.954	-5.3%	17.415	16.320	-6.7%
5%	13.215	12.523	-5.5%	18.854	17.670	-6.7%

Bottom hole temperature (BHT) was also determined using software. Well depth used was obtained from the prospected Total SA's well depth of 3.633km. The value obtained was compared with Figure 38 below data.

	Temperature Gradient (°F/100 ft Depth [°C/100 m Depth])					
	1.6 [0.9]	2.0 [1.1]	2.4 [1.3]	2.7 [1.5]	3.1 [1.7]	3.5 [1.9]
Depth[4] (ft [m])	BHCT[5] (°F [°C])					
1,000 [305]	80 [27]	80 [27]	80 [27]	80 [27]	80 [27]	80 [27]
2,000 [610]	89 [32]	89 [32]	90 [32]	90 [32]	91 [33]	91 [33]
4,000 [1,020]	99 [37]	100 [38]	101 [38]	102 [39]	103 [39]	104 [40]
6,000 [1,830]	112 [44]	114 [46]	116 [47]	118 [48]	120 [49]	126 [52]
8,000 [2,440]	126 [52]	129 [54]	135 [57]	140 [60]	146 [63]	160 [71]
10,000 [3,050]	141 [61]	146 [63]	158 [70]	167 [75]	180 [82]	200 [93]
12,000 [3,660]	148 [64]	165 [74]	183 [84]	201 [94]	219 [104]	236 [113]
14,000 [4,270]	164 [73]	185 [85]	207 [97]	228 [109]	250 [121]	271 [133]
16,000 [4,880]	182 [83]	207 [97]	233 [112]	258 [126]	284 [140]	309 [154]
18,000 [5,490]	201 [94]	231 [111]	261 [127]	291 [144]	321 [161]	350 [177]
20,000 [6,100]	222 [106]	256 [124]	291 [144]	326 [163]	360 [182]	395 [202]
22,000 [6,710]	244 [118]	284 [140]	324 [162]	364 [184]	404 [207]	444 [229]

Figure 39. BHCT for casing well simulation tests (Nelson & Dominique, 2006)

Software results gave 94.03˚C (shown in Appendix C2) while Figure 38 above shows the closest value of 113˚C, assuming temperature gradient of 1.9˚C/100m.

Figure 3 production casing was used to illustrate Figure 6 and 7 casing standoff; the software also helped to determine the size of centralizer as well as annular gaps assuming minimum STO of 75%. Results are shown in Appendix C3. The software simplifies complex drilling calculations and allows quick determination of parameters needed.

CHAPTER 6: CONCLUSIONS AND RECOMMENDATIONS

6.1 Conclusions

Designing cement slurry that would be suitable for wellbore conditions largely depends on the clinker manufacturing process. The raw materials used for clinker manufacturing were optimized to obtain the best desired clinker quality acceptable by API standards. The clinker used to make a Class G cement had C3S of 65%, C3A of 6.9% within burning conditions suitable to make a required free lime of 1.5%. The cement slurries designed using bentonite and durapozz additives had acceptable C3S and C3A for 1% Durapozz slurry, as well as 1 and 3% Bentonite slurries.

As dosage of both additives was increased, density became lower. The lower the density the lower the cost of the cement slurry prepared with Durapozz as durapozz additive costs much lesser than bentonite additive. The slurry density target drives the cost of additives. They are used in well cements to achieve a desired density with specific performance criteria. All the cement slurries prepared were lightweight slurries with densities between 1500- 1700kg/m3. Lightweight slurries are used in areas with low formation pressure; it would be suitable on the surface of a wellbore up to 1830 m. Durapozz slurries were denser than Bentonite slurries due to their wider range of particle size distribution which allowed better packing ability than Bentonite slurries. Therefore Durapozz slurries would be less porous than Bentonite slurries; this has an advantage of limiting harsh wellbore environments from destructing the cement slurry.

The investigations revealed that the proposed lightweight cement has less than 5.9% free water content and acceptable compressive strength >2.1MPa. However, thickening times for DZ were not within acceptable limits therefore it can be used as OWC slurry in place of Bentonite provided dosages are kept below 5% substitution. Durapozz was found to act as a thickening time accelerator at low dosages and retarder at high dosages, whilst bentonite showed acceleration of thickening time as dosage was increased. Using DZ at high doses may cause blockages in the annular of the wellbore as shown by thickening time decreasing. Both additives need to be investigated when mixed with other additives to obtain slurry within specified thickening times.

At lower dosages, high temperature may affect late strength. Early strength not affected by temperature at lower dosages for DZ slurries. Disadvantages of bentonite slurry are their low resistance to much high temperatures. Addition of more BT into the slurry reduces its pumping at 23 ˚C. This reaction needs to be investigated at much higher temperatures and increased w/c ratio to see how thickening time and rheology behaves.

The Bingham plastic model was determined to be best fit for all the Durapozz slurries and not the power model as shown by higher correlation coefficient. All slurries prepared are shear-thinning slurries, which means the slurries would be able to flow in the annulus of wellbore. Viscosity increases with time, beginning from mixing with water, because of the chemical reaction of setting. When the viscosity becomes too great, the slurry does not flow. The apparent viscosity of DZ slurries decreases with the continuance of shearing, when fluid is sheared at a constant rate, this behavior shows it is a thixotropic fluid. The rheology results were inputted in PVI drilling software (Appendix C) and it showed that n and plastic viscosity were the same, however K and yield stress showed slight differences and acceptable error below 7%.

To use durapozz, a form of activation is often required, for example, mechanical activation through grinding. If this can be done then substitution can go to as high as possible, thereby creating a low-carbon footprint slurry.

6.2 Recommendations

Effect of used temperature on compressive strength only was not enough; other variables such as effect of temperature on viscosity needs to be investigated at higher temperatures up to about 94˚C as this was the formation temperature determined by drilling software.

The API standard used was adequate, more recent standard procedure to be used always if accessible as there may be differences from the last published API standard specification, for example previous standards used to define Class E and F and on later standards this was removed due to the fact that some of these cements reacted with the additives.

Durapozz additive has a potential of being used as accepted Oil Well Cement Slurry, more investigations still need to be done at finer dosages. This would assist in reducing the carbon tax costs caused by emissions of carbon dioxide from production of cement.

Fluid loss to be also investigated at different temperatures and different Durapozz dosages in order to assess how density as well as rheology is affected by loss of fluid.

Stability of Durapozz when mixed with other required additives still needs to be investigated, this is important as environmental requirements of a well will demand different additives to be used in different dosages.

Other rheological models stated in Appendix A need to be tested and the best correlating model selected and justified.

7. REFERENCES

1. Agwu, O. E. et al., 2021. A critical review of drilling mud rheological models. *Journal of Petroleum Science and Engineering,* 203(108659), pp. 1-21.

2. Ahmed,Nazeer, 2014. *Hydraulics of Wells.* Virginia: American Society of Civil Engineers.

3. Aird, P., 2019. Deepwater Pressure Management. In: *Deepwater Drilling.* s.l.:s.n.

4. Anaele, J. & Otaraku, I., 2020. Effect of Temperature on the Thickening Time Property of Cement Slurry. *THE INTERNATIONAL JOURNAL OF SCIENCE AND TECHNOLOGY,* 8(3), pp. 52-54.

5. Anjuman, S. & Nehdi, L. M., 2012. Rheological properties of oil well cement slurries. *Construction Materials,* 165(CM1), pp. 25-44.

6. Bennett, T., 2016. Well Cement Integrity and Cementing Practices. *Australia: University of Adelaide*.

7. Bett, K. E., 2010. Geothermal well cementing,materials and placement techniques. *Geothermal Training Programme,* 9(10), pp. 99-130.

8. Broni-Bediako, E., Joel F, O. & Ofori-Sarpong, G., 2016. Oil Well Cement Additives: A Review of the Common Types. *Oil and Gas Research ,* 2(1), pp. 1-7.

9. Broni-Bediako, E., Joel, O. & Ofori-Sarpong, G., 2015. Comparative Study of Local Cements with Imported Class 'G' Cement at. *Journal of Petroleum & Environmental Biotechnology,* 6(4), pp. 1-7.

10. Broni, B., Joel, O. & Ofori, S., 2015. Comparative study of local cements with imported class G cement at different temperatures for oil well cementing operations in Ghana. *Journal of Petroleum & Environmental Biotechnology,* 6(4), pp. 1-7.

11. Cement, L. G. O. a. G. &. L. I. P., 2014. *Well Cement.* USA,Brazil,Western Canada,Malaysia,Spain: Lafarge .

12. Crook, R. & Halliburton, 2006. Cementing. In: R. F. Mitchell, ed. *Petroleum Engineering Handbook.* Halliburton: Society of Petroleum Engineers, pp. 369-431.

13. DeBruijn, G. and Whitton, S.M., 2021. Fluids. In *Applied Well Cementing Engineering* (pp. 163-251). Gulf Professional Publishing.

14. Devold, H., 2013. *Oil and gas production handbook An introduction to oil and gas production,transport,refining and petrochemical industry.* 3 ed. Oslo: ABB Oil and Gas.

15. Falode, O. A., Salam, K. K., Arinkoola, A. O. & Ajagbe, B. M., 2013. Prediction of compressive strength of oil field class G cement. *Journal of Petroleum Exploration and Production Technology,* 10(7), pp. 1-8.

16. Finger, J. & Doug, B., 2010. Overview of Geothermal Drilling. In: N. Jay, ed. *Handbook of Best Practices for Geothermal Drilling.* Limited ed. California: Sandia National Laboratories, pp. 16-17.

17. Guner, D. & Ozturk, H., 2015. *Comparison of Mechanical Behavior of G Class Cements for different Curing.* Ankara, 24th International Mining Congress and Exhibition of Turkey.

18. Hossain, M.E. and Al-Majed, A.A., 2015. *Fundamentals of sustainable drilling engineering*. John Wiley & Sons.

19. Johannesburg Stock Exchange, 2019. *South African Markets Insight.* [Online] Available at: https://www.southafricanmi.com/crude-oil-imports-prices-30may2019.html [Accessed 29 March 2020].

20. Juenger, M. C. G. & Siddique, R., 2015. Recent advances in understanding the role of supplementary. *Cement and Concrete Research,* 78(1), pp. 71-80.

21. Kaduku, T., 2015. *The use of South African coal fly ash(CFA) as an additive to oil well cementing during cementing operations,* Johannesburg: Kaduku,Tendai.

22. Krakowiak, K. J. et al., 2015. Nano-chemo-mechanical signature of conventional oil-well cement. *Cement and Concrete Research,* 67(1), pp. 103-121.

23. Kremieniewski, M., 2020. Recipe of Lightweight Slurry with High Early Strength of the Resultant Cement Sheath. *Energies,* 1583(13), pp. 1-13.

24. Kremieniewski, M., 2020. Ultra-Lightweight Cement Slurry to Seal Wellbore of Poor Wellbore Stability. *energies,* 13(3124), pp. 1-18.

25. Larki, O.-A., Apourvari, S. N., Schaffie, M. & Farazmand, R., 2019. A new formulation for lightweight oil well cement slurry using a natural pozzolan. *Advances in Geo-Energy Research,* 3(3), pp. 242-249.

26. Lavrov, A., 2016. *Effect of eccentric annulus,washouts and breakouts on well cement quality:Lamina regime.* Trondheim, Energy Procedia.

27. Leusheva, E., Brovkina, N. & Morenov, V., 2021. Investigation of Non-Linear Rheological Characteristics of Barite-free drilling fluids. *fluids,* 6(327), pp. 1-12.

28. Li, H. et al., 2021. Rheological behaviors of cement pastes with multi-layer graphene. *Construction and Building Materials,* 269(121327), pp. 1-10.

29. Looyeh, R. & Bernt, A. S., 2019. Drilling Design and Selection of Optimal Mud Weight. In: *Petroleum Rock Mechanics.* s.l.:Elsivier, p. 2nd Edition.

30. Lota, J. S., K, L. & R, F. S., 2013. *API Standard Class G Cement and Its Inconsistencies in Slurry Thickening Times.* Wartford, 289033144.

31. Lota, J.S., 1993. *The hydration of class G oilwell cement* (Doctoral dissertation, Imperial College London (University of London)).

32. Lozhechnikova, A., 2011. *DETERMINATION OF SLURRY´S VISCOSITY USING CASE BASED REASONING APPROACH,* s.l.: LAPPEENRANTA UNIVERSITY OF TECHNOLOGY.

33. Mayne, W., 2018. *Manual on Subsurface Investigations,* Georgia: National Academy of Sciences.

34. Mbedi, 2018. *Africa:oil and gas refining.* [Online]
Available at: https://mbedi.co.za/indy/oilg/ogrf/af/p0005.htm
[Accessed 14 April 2020].

35. Merah, A. and Krobba, B., 2017. Effect of the carbonatation and the type of cement (CEM I, CEM II) on the ductility and the compressive strength of concrete. *Construction and Building Materials*, *148*, pp.874-886.

36. Moradi, S. S. T. & Nikolaev, N. I., 2017. Fre e fluid control of oil well cements using factorial design. *Journal of Engineering Research,* 5(1), pp. 220-229.

37. Munjal, P., Hau, K. K., Prabhakar, A. & Hon, C. C., 2019. Oil Well Cement for high temperature-A review. *IOP Conference Series: Materials Science and Engineering,* 652(1), pp. 1-6.

38. Nelson, B. E. & Dominique, G., 2006. *Well cementing.* 2nd ed. Texas: Schlumberger.

39. Pichtel, J., 2016. Oil and Gas Production Wastewater: Soil Contamination and Pollution Prevention. *Natural Resources and Environmental Management,* 2016(2707989), pp. 5-6.

40. Piklowska, A., 2017. Cement slurries used in drilling. *World Scientific News*, 18 May, pp. 151-152.

41. Pinka, J. & Kucirkova, L., 2015. THE IMPORTANCE OF THE FORMATION AND FRACTURE PRESSURES FOR THE SELECTION OF THE DEPTHS FOR CASING SETTING IN SLOVAKIA. *AGH DRILLING,OIL,GAS,* 32(2), pp. 381-394.

42. Rompetrol well services, 2018. *Rompetrol well services.* [Online]
Available at:
https://rompetrolwellservices.kmginternational.com/en/services/cementing-software
[Accessed 23 May 2020].

43. Rzepka, M. et al., 2016. Recipes of cement slurries for sealing casing in deep wellbores. *AGH Drilling oil and gas,* 33(2), pp. 455-469.

44. Salam, K. K., Arinkoola, A. O., Ajagbe, B. M. & O, S., 2015. MODELING OF RHEOLOGICAL PROPERTIES OF CLASS G CEMENT SLURRY. *Petroleum and Coal,* 57(5), pp. 447-465.

45. Tang, Y., Gao, J., Liu, C., Chen, X. and Zhao, Y., 2019. Dehydration pathways of gypsum and the rehydration mechanism of soluble anhydrite γ-CaSO4. *ACS omega*, *4*(4), pp.7636-7642.

46. Thetford, K., 2013. *The Atlantic,Understanding how we produce and use petroleum.* [Online]
Available at:
https://www.theatlantic.com/technology/archive/2013/08/turning-crude-oil-into-the-stuff-we-use/278680/
[Accessed 12 April 2020].

47. Total South Africa, 2019. *Total.* [Online]
Available at:
https://www.total.com/en/media/news/press-releases/total-makes-significant-discovery-and-opens-new-petrolem-province-offshore-south-africa
[Accessed 16 April 2020].

48. Yergin, D., 2011. Petroleum. In: *The Quest* . s.l.:Penguin Books , p. 137.

49. Yuan, Z., 2012. *Effect of mechanical properties and reservoir compaction on HTHP well integrity,* Texas: Yuan,Zhaogaung.

APPENDIX A: Rheological Models

Model	Correlation and possible deficiencies
Bingham plastic model [2 parameter model] Year of development: 1916	$\tau = \tau_o + \mu_p\gamma$ Where $PV(\mu_p) = \theta_{600} - \theta_{300}$ $YP(\tau_y) = \theta_{300} - \mu_p$ $AV = \theta_{600}/2$ *Deficiencies*: (i) Deviates from data at high temperatures (Shah et al., 2010). (ii) For drilling muds, this model does not accurately describe the mud's flow behaviour at low-shear-rates (Guo and Liu, 2011; Shakers, 2005; Adewale et al., 2017) (iii) This model has the tendency to overestimate the yield stress of mud (Huang et al., 2019)
Casson model [2 parameter model] Year of development: 1959	$\tau^{\frac{1}{2}} = \tau_o^{\frac{1}{2}} + (\mu_o\gamma)^{\frac{1}{2}}$ *Deficiencies*: i. Rarely applied to drilling muds (Baker Hughes, 2006). Applied to cement slurry characterisation and is better for estimating viscosities at high shear rate when only low and intermediate shear-rate data are available (Ochoa, 2006) ii. Cannot estimate maximum shear stress limit but can estimate infinite shear stress limit (Afolabi et al., 2017) iii. The physical significance of its rheological parameters is not very clear (Huang et al., 2019)
Ostwald-de-Waele or Power law model [2 parameter model] Year of development: 1923, 1925	$\tau = k\gamma^n$ Where $n = 3.32\ log\left(\frac{\theta_{600}}{\theta_{300}}\right)$ and $k = \frac{\theta_{600}}{1022^n}$ *Deficiency*: Does not account for the yield stress of drilling muds leading to inaccurate results (Netwas Group Oil, 2020a; Huang et al., 2019)
Heinz – Casson model Year of development: 1959	$\tau^n = (\gamma_0)^n + k(\gamma)^n$ *Deficiency*: has very limited application in characterizing the viscoplastic behaviour of fluids in the petroleum industry (Song et al., 2006)
Ellis Model [3 parameter model] Year of development: 1967	$\tau = [\mu_0/\{1 + (\tau/\tau_{1/2})^{\alpha-1}\}]\gamma$ Where $\tau_{1/2}$ is the value at which $\mu_a = \frac{\mu_o}{2}$; $(\alpha - 1)$is the slope of line obtained when $\left[\left(\frac{\mu_o}{\mu_a} - 1\right)\right]$ is plotted against $\frac{\tau}{\tau_{1/2}}$ on a log-log scale *Deficiency*: The mathematical complexity of the model makes it cumbersome to determine model parameters (Shah et al., 2010)

Sisko model [3 parameter model] Year of development: 1958	$\tau = K_1\gamma + K_2\gamma^n$ where K_1 is the coefficient of viscosity, K_2 is the consistency coefficient and n is the flow index of the fluid. $n < 1$ represents a pseudoplastic (shear thinning) fluid, $n > 1$ represents a dilatant (shear thickening) fluid and $n = 1$ correspond to a Newtonian fluid *Deficiency*: Cannot estimate maximum shear stress limit but can estimate infinite shear stress limit (Afolabi et al., 2017)
Herschel-Bulkley model [3 parameter model] Year of development: 1926	$\tau = \tau_o + K(\gamma)^n$ *Deficiency*: Challenges exist in performing hydraulic calculations due to the extra rheological parameter (Baker Hughes, 2006; Huang et al., 2019)
Robertson-Stiff model [3 parameter model] Year of development: 1976	$\tau = K(\gamma + \gamma_o)^n$ *Deficiencies*: Rarely used in the drilling fluid industry because of the complexity in evaluating the three parameters (Ochoa, 2006; Ohen and Blick, 1990); Limited usage in the field due to the tedious nature of the flow function (Bailey, 1996)
Casson – Steiner model [3 parameter model] Year of development: 1958	$\tau = \left(\frac{2}{1+A}\sqrt{\tau_y} + \sqrt{\mu_c\gamma}\right)^2$ *Deficiency*: Limited usage in the field due to the tedious nature of the flow function (Bailey, 1996)

Model	Correlation and possible deficiencies
Collins-Graves [3 parameter model] Year of development: 1978	$\tau = (\tau_y + k\gamma)(1 - e^{-\beta\gamma})$ *Deficiency*: Limited usage in the field due to the tedious nature of the flow function (Bailey, 1996)
Cross model [4 parameter model] Year of development: 1965	$\tau = \gamma\left(\mu_\infty + \frac{\mu_o - \mu_\infty}{1 + \alpha\gamma^{2/3}}\right)$ *Deficiency:* Due to the mathematical complexity of the model arising from the high number of parameters, it is tedious to determine model parameters (Shah et al., 2010)
Carreau Model [3 parameter model] Year of development: 1972	$\tau = \frac{\mu_c\gamma}{(1 + \gamma/\gamma_c)^A}$ *Deficiency:* This model is mainly used for food and beverages (Steffe, 1996) and blood flow (Shibeshi and Collins, 2005)
Modified Robertson-Stiff model [3 parameter model]	$\tau = \tau_O + K(\gamma_O + \gamma)^n$ *Deficiency*: Relative complexity in determining the model parameters (Ochoa, 2006)
Reiner model [3 parameter model] Year of development: 1930	$\gamma = \tau\left[\mu_\infty + \frac{\mu_o - \mu_\infty}{1 + (\tau/\tau_y)}\right]^{-1}$ *Deficiency:* Limited usage in mud calculations due to its complexity (Bui and Tutuncu, 2016)
Prandtl-Eyring model [2 parameter model] Year of development: 1928, 1936	$\tau = A_t Sinh^{-1}\left(\frac{\gamma}{B_p}\right)$ *Deficiency*: Limited usage in mud calculations due to its complexity (Bui and Tutuncu, 2016)
Gucuyener Model [3 parameter model] Year of development: 1983	$\tau = \sqrt[n]{\tau_y + \mu_G\sqrt{\gamma}}$ *Deficiency*: Not reported
Carreau-Gahleitner Model [3 parameter model] Year of development: 1991	$\tau = (\sqrt{\tau_y} + \sqrt{\mu_c\gamma})^A$ *Deficiency*: The model does not always give a good fit to mud rheology data and this adversely affects the results of hydraulic calculations (Bui and Tutuncu., 2016)
Vipulanandan model [2 parameter model] Year of development: 2014	$\tau = \tau_O + \frac{\gamma}{A + D\gamma}$ *Deficiency*: Not reported
Hyperbolic model [4 parameter model] Year of development: 1996	$\tau = \tau_y + A\sqrt{\left(\frac{\gamma - \gamma_{cp}}{B}\right)^2 - 1}$ *Deficiency*: Unsuitable for general application due to the instability of the implicit solutions for the complex expressions of this model (Bailey, 1996)

Tscheuschner model [4 parameter model] Year of development: 2006	$\tau = \tau_y + A\gamma + B\gamma^C$ *Deficiency*: Limited use due to the complexity of the resulting flow equations caused by the high number of model parameters (Kelessidis and Maglione, 2006).
Rational polynomial Year of development: 2001	$\tau = \frac{P_0 + P_1\gamma + P_2\gamma^2 + \ldots\ldots + P_k\gamma^k}{1 + Q_1\gamma + Q_2\gamma^2 + \ldots\ldots + Q_m\gamma^m}$ *Deficiency*:Evaluating the constants in the model is cumbersome

APPENDIX B: Rheology Calculations

Slurry at 1% bentonite				
Dial Reading(rpm)	**Ramp up**	**Ramp down**	**Reading Ratio**	**Averege Reading**
3	26	38	0.684210526	32
6	36	39	0.923076923	37.5
100	51	54	0.944444444	52.5
200	64	68	0.941176471	66
300	76	81	0.938271605	78.5

τpower	**τbingham**	**error-power**	**error-bingham**
16.37695	18.144664	0.2%	11.0%
18.48002	18.374327	-3.5%	-4.1%
30.17663	25.57045	12.5%	-4.7%
34.05182	33.2259	1.0%	-1.5%
36.54542	40.88135	-8.9%	1.9%

corr coeff-power	**corr coeff bingham**
0.969221	0.9919853

Shear Rate,γ̆	**Shear Stress,τ**
5.115	16.3488
10.23	19.15875
170.5	26.82225
341	33.7194
511.5	40.10565

Slurry at 3% DZ				
Dial Reading(rpm)	**Ramp up**	**Ramp down**	**Reading Ratio**	**Averege Reading**
3	28	30	0.933333333	29
6	37	39	0.948717949	38
100	51	54	0.944444444	52.5
200	63	67	0.940298507	65

300	75	80		77.5

τpower	τbingham	error-power	error-bingham
15.59254	17.645687	5.2%	19.1%
17.71850	17.876373	-8.7%	-7.9%
29.76705	25.10455	11.0%	-6.4%
33.82562	32.7941	1.9%	-1.2%
36.45163	40.48365	-7.9%	2.2%

corr coeff-power	corr coeff bingham
0.972259	0.9821165

Shear Rate,ў	Shear Stress,τ
5.115	14.8161
10.23	19.4142
170.5	26.82225
341	33.2085
511.5	39.59475

Slurry at 5% Durapozz				
Dial Reading(rpm)	Ramp up	Ramp down	Reading Ratio	Averege Reading
3	31	33	0.939393939	32
6	40	42	0.952380952	41
100	51	55	0.927272727	53
200	63	67	0.940298507	65
300	74	78	0.948717949	76

Shear Rate,ẙ	Shear Stress,τ
5.115	16.3488
10.23	20.9469
170.5	27.0777
341	33.2085
511.5	38.8284

τpower	τbingham	error-power	error-bingham
17.16423	19.061669	5.0%	16.6%
19.18003	19.269338	-8.4%	-8.0%
30.10159	25.7763	11.2%	-4.8%
33.63678	32.6986	1.3%	-1.5%
35.89420	39.6209	-7.6%	2.0%

corr coeff-power	corr coeff bingham
0.96674	0.9803721

APPENDIX C: PVI Drilling Software

1. Rheology

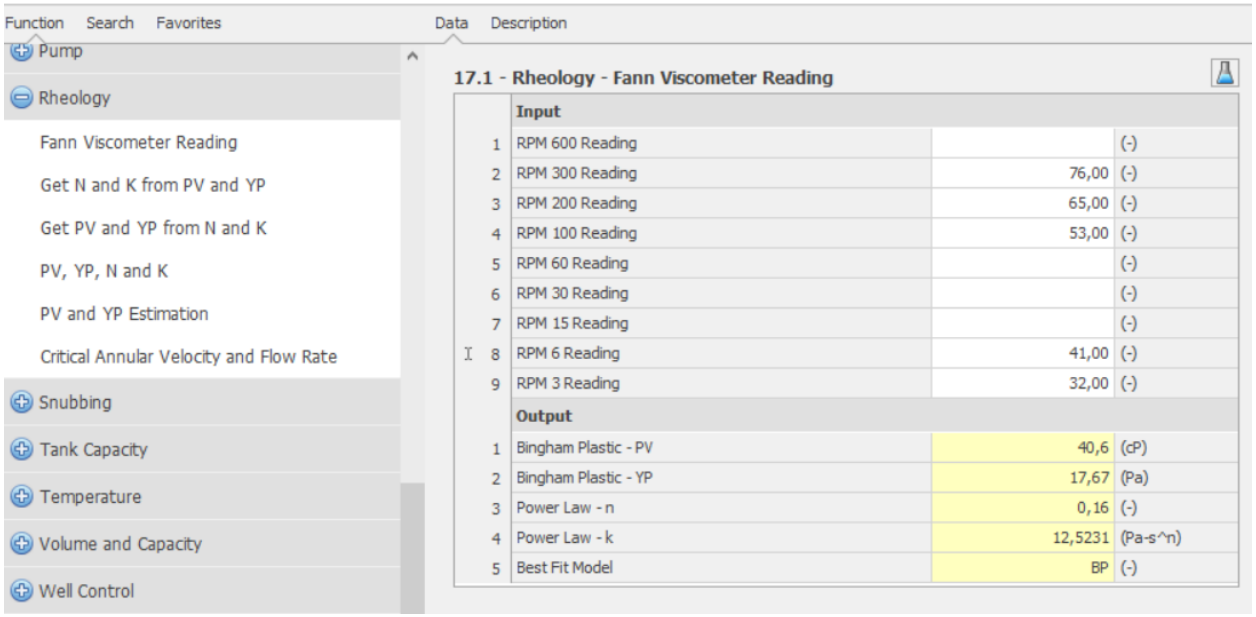

2. Formation Temperature

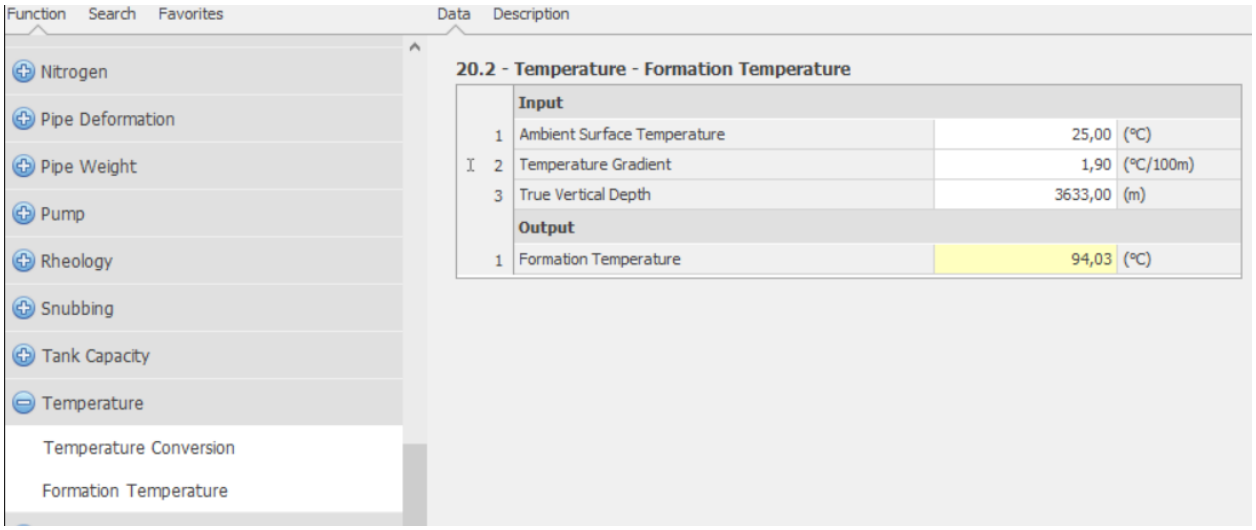

3. Standoff Casing Centraliser